Title: Revisiting the Hewlett and Hibbert (1963) hillslope drainage experiment and modeling effects of decadal pedogenic processes and leaky soil boundary conditions

Authors: Raymond M. Lee[1], Kevin J. McGuire[1,2], Brian D. Strahm[1], Jennifer D. Knoepp[3], C. Rhett Jackson[4], and Ryan D. Stewart[5]

[1]Department of Forest Resources and Environmental Conservation, Virginia Tech, Blacksburg, VA 24061, USA.

[2]Virginia Water Resources Research Center, Virginia Tech, Blacksburg, VA 24061, USA.

[3]Coweeta Hydrologic Laboratory, USDA Forest Service, Otto, NC 28763, USA.

[4]Warnell School of Forestry and Natural Resources, University of Georgia, Athens, GA 30602, USA.

[5]School of Plant and Environmental Sciences, Virginia Tech, Blacksburg, VA 24061, USA.

Corresponding author: Raymond M. Lee (raylee@vt.edu)

Key Points:

- Seminal drainage experiment in hillslope model repeated after 55 y of pedogenesis, and similar drainage pattern observed for first ~10 d
- Changes in soil physical properties did not lead to changes in hydraulic properties
- Leakage from bottom of experimental model, representative of natural conditions, largely shortened drainage duration

Abstract

Subsurface flow dominates water movement from hillslopes to streams in most forested headwater catchments. Hewlett and Hibbert (1963) constructed an idealized hillslope model (0.91 × 0.91 × 15.0 m; 21.8°) using reconstituted C horizon soil to investigate importance of interflow, a type of subsurface flow. They saturated the model, covered it to prevent evaporation, and allowed free drainage for 145 d. The resulting recession drainage curve suggested two phases: fast drainage of saturated soil in the first 1.5 d, then slow drainage of unsaturated soil.

Hydrologists interpreted the latter as evidence interflow could sustain baseflow, even during extended drought. Since that experiment, typical forest vegetation grew in the model, providing root and litter inputs for 55 years. We removed all above-ground live biomass and repeated the experiment physically and numerically (HYDRUS-2D), hypothesizing that pedogenesis would change the drainage curve and further elucidate the role of unsaturated flow from hillslopes. Contrary to this hypothesis, drainage curves in our twice-repeated physical experiments and numerical simulation were unchanged for the first ~10 days, indicating pedogenesis and biological processes had not largely altered bulk hydraulic conductivities or soil moisture release characteristics. However, drainage unexpectedly ceased after about two weeks (14.3 ± 2.52 d), an order of magnitude sooner than in the original experiment, due to an apparent leak in the hillslope analogous to commonly observed bedrock fractures in natural systems. Thus, our results are a more natural recession behavior that highlights how incorporation of alternative hydrologic outputs can reduce drainage duration and volume from soils to baseflow.

Keywords: hillslope hydrology; Variable Source Area; interflow; baseflow; HYDRUS-2D

1 Introduction

Water movement from hillslopes to streams is dominated by subsurface processes in forested headwater catchments. Shallow lateral subsurface flow is initiated when infiltrating precipitation flows through permeable soil near parallel to the slope, often above an impeding layer (Chorley, 1978). This lateral downslope flow can occur as unsaturated flow (Zaslavsky & Sinai, 1981), saturated flow (Whipkey, 1965), or saturated macropore flow (e.g. Beven & Germann, 1982). As unsaturated flow in a sloping soil, the downslope lateral component depends on the degree of soil anisotropy (Zaslavsky & Rogowski, 1969). Hewlett and Hibbert's experimental hillslope work (Hewlett, 1961a; Hewlett & Hibbert, 1963) showed that after precipitation has ceased and the saturated zone has contracted, hydraulic head gradients can move unsaturated soil water laterally from upslope soils both in large volumes and over an extended recession flow drainage period, thereby sustaining baseflow between storms.

Hewlett and Hibbert's interest in such sustained baseflow was motivated by observations in the mountainous terrain of the Coweeta Hydrologic Laboratory in the Blue Ridge mountains of North Carolina. Here, perennial streams are not supported by large valley aquifers, though baseflows are sustained during long periods without rain. To determine if unsaturated interflow could explain this paradox, Hewlett and colleagues built experimental hillslope models, which were inclined concrete structures filled with locally-sourced and reconstituted (i.e., homogenized and repacked) C horizon (sandy clay loam) forest soil, then conducted drainage experiments to mimic matrix flow over zero-conductivity bedrock. In the 1963 study, Hewlett and Hibbert saturated a model (0.91 × 0.91 × 15.0 m; 21.8° [40 %] slope), then covered the soil to prevent evaporation and allowed the model to drain until it no longer yielded water (145 d). From this

79 experiment they developed a drainage curve used to argue that there were two phases of
80 drainage: fast drainage of the saturated portion of the hillslope (for 1.5 d), then slow drainage of
81 unsaturated soil (see Fig. 2 in Hewlett and Hibbert 1963).
82
83 These observations of long-duration drainage of unsaturated sloping soils have been highly
84 influential in shaping our understanding of the role of soil water, as opposed to groundwater, in
85 supplying water to headwater streams even in periods of extended drought. For example, long-
86 duration recession flow through unsaturated soil, as described in Hewlett and Hibbert's work, is
87 widely observed (McGuire & McDonnell, 2010; Moore, 1997; Mosley, 1979; Post & Jones,
88 2001; Rothacher, 1965; Weyman, 1973) and informs many conceptual models (Bonell, 1998;
89 Dunne, 1983; Genereux & Hemond, 1990; Harr, 1977; Kirkby, 1988; McGlynn & McDonnell,
90 2003; Nippgen et al., 2015; Scholl & Hibbert, 1973; Torres et al., 1998). Furthermore, Hewlett
91 and Hibbert observed that the area supplying baseflow is not constant but expands or shrinks in
92 response to interactions among precipitation, recharge, and soil moisture, which led to their
93 development of the Variable Source Area concept (VSA; Hewlett, 1961b, Hewlett & Hibbert,
94 1967). The VSA concept, which is the foundation for physically-based catchment models (e.g.,
95 TOPMODEL [Beven & Kirkby, 1979; Golden et al., 2014; Wolock & McCabe, 1995]; Soil
96 Moisture Routing model [Frankenberger et al., 1999]; and CN-VSA [Lyon et al., 2004]), informs
97 many studies and continues to be refined decades after the concept was conceived (Ambroise,
98 2004; Bernier, 1985; Dunne, 1983; Nippgen et al., 2015; Ward, 1984; Weiler et al., 2005).
99
100 However, the drainage curve produced from the idealized hillslope model in the study by
101 Hewlett and Hibbert (1963) may not reflect processes in hillslopes with heterogeneous natural

soil. The soil profile in their model was texturally and structurally homogenous, a simplification that neglected exponential declines in saturated hydraulic conductivity and porosity often found in natural hillslopes (e.g., Ameli et al., 2016; Beven, 1982; Elsenbeer, 2001). Another limitation was absence of vegetation and organic matter in the soil surface, which, if present, would increase soil water retention, as organic matter is strongly correlated with soil water content at saturation (Ankenbauer & Loheide, 2016). Not incorporating organic matter provided more control for isolating mechanisms affecting drainage but did not replicate natural conditions. Furthermore, the lower boundary of the model, representing the soil-bedrock interface, was linear (i.e., straight and without complex microtopography) and impermeable, which is uncharacteristic of weathered bedrock in many hillslopes that may have both primary permeability and fractures (Appels et al., 2015; Freer et al., 2002; Gabrielli et al., 2018; Hale & McDonnell, 2016; Klaus & Jackson, 2018; Pfister et al., 2017).

These simplifications in the flow domain and boundary conditions likely impacted movement of water into, through, and out of the hillslope model. Analytical and numerical models have replicated the experiment and estimated outflow adequately, though these studies incorporated the abovementioned simplifications (Sloan & Moore, 1984; Stagnitti et al., 1986; Steenhuis et al., 1999; Zecharias & Brutsaert, 1988). Thus, what is truly needed to advance our understanding of the relationship between hillslope soil moisture and baseflow is a more realistic set of field observations and modeling exercises that more accurately represent the physical properties of the subsurface.

Fifty-five years passed since Hewlett and Hibbert (1963) conducted their seminal experiment,

and since then pedogenic processes (e.g., organic matter addition, bioturbation, aggregation, settling, weathering, and erosion) had visibly changed soil properties in the hillslope model from the original experiment to a condition that was closer to those in adjacent natural forest soils. For example, trees (up to 40 cm ground line diameter) grew inside the model, a thin A horizon developed, and invertebrates (e.g., ants and worms) colonized the soil. We expected from past research on macropores and near-surface hydrologic processes (Beven & Germann, 1982; Clothier et al., 2008; Hendrickx & Flurry, 2001) that this tree growth and root development would create macropores that would substantially alter bulk saturated conductivities, soil moisture release curves, and, consequently, drainage behavior of the soil. We were particularly interested in whether and how such soil development may have impacted the drainage curve compared to the original observations of Hewlett and Hibbert (1961a; 1963) due to the subsequent broad-scale interpretations of hillslope subsurface flow dynamics that have been made from their work.

In this study we returned to the hillslope model used in the 1963 study and, after removing all above-ground live biomass, characterized the soil for horizonation, bulk density, texture, carbon content, water retention, and saturated hydraulic conductivity. Then, we performed two repetitions of the Hewlett and Hibbert (1963; hereafter referred to as the original) drainage experiment, which were complemented by investigations with a 2-D dynamic numerical model based on Richards's equation (Richards, 1931). We also conducted irrigation and tracer experiments to examine drainage and hydrologic mass balance. We aimed to answer the following research questions: Have soil properties changed in the 55 years between experiments, and did those changes affect water retention and recession dynamics?

2 Methods

2.1. Physical experiment

2.1.1. Physical hillslope soil model

The hillslope soil model (described above) was located at the Coweeta Hydrologic Laboratory (hereafter Coweeta), a USDA Forest Service experimental forest, and consisted of two segments. The toeslope segment was level, extending 0.3 m, in which a water table was maintained by an outlet pipe at a height of 0.46 m above the ground at the base of the trough (Fig. 1; Hewlett & Hibbert, 1963). The hillslope segment was packed with 10.85 m^3 of sieved (6.4 mm) C horizon soil (Saunook series; fine-loamy, mixed, superactive, mesic Humic Hapludults [Soil Survey Staff, 2019]; formerly known as Halewood) that was excavated nearby. The sandy clay loam soil was homogenized and packed to a bulk density of 1.3 g cm^{-3}, averaging 60 % sand, 18 % silt, and 22 % clay. Soil graded to sand and gravel at the toe of the slope to simulate gravelly stream bank conditions (Hewlett & Hibbert, 1963).

In 2012, four trees (Fig. 1) that had grown in the model were cut a few centimeters above the ground line and removed, leaving the root structure intact within the soil. In 2015, the model was covered by a curved shelter, which was ~2 m above the ground surface at its peak and was open at the upslope and downslope ends, allowing airflow across the soil surface and gas exchange between the soil and atmosphere. The shelter was made of laminated reinforced polyethylene film, which prevented meteoric water input while allowing transmission of 83 % of incoming diffuse visible light. The model was maintained in a devegetated state with herbicide (glyphosate), and leaf litterfall was collected once per year at the end of autumn from the forest floor nearby (over an area equal to the surface of the model), and added to the surface of the

model. In Dec 2016, we conducted the first repetition of the drainage experiment, which was followed by another in Feb 2017 and a steady-state irrigation experiment in Jun 2017.

2.1.2. Drainage experimental setup

We repeated the drainage experiment as described in Hewlett and Hibbert (1963) twice to confirm reproducibility. To initialize the hillslope model for each experiment, we irrigated the model using sprinklers (Fig. 1a) for at least 20 d (14.3 mm d^{-1}; 196 L d^{-1}) until we reached hydrologic steady state, then we added water by hand to near-saturation (i.e., wet-up period). In both water additions by hand, we added 1,500 L of water evenly across the surface (~1.6 cm h^{-1} for 7 h in the first experiment and ~1.2 cm h^{-1} for 9 h in the second) until soil water content across the hillslope was 42.9 % in the first experiment and 43.6 % in the second, and the rate of outflow (Q_{out}; L d^{-1}) plateaued. These were similar to initial conditions at the start of the original experiment (Hewlett & Hibbert, 1963). Immediately after water additions, a plastic tarp was placed on the soil to prevent evaporation, and free drainage was allowed to occur for 60 and 48 d in each respective experiment (well past the time Q_{out} had ceased).

2.1.3. Steady-state irrigation mass balance experimental setup

Drainage curve results from our experiments suggested there was a possible leak in the hillslope model. To confirm presence and estimate magnitude of a leak, two mass balances (hydrologic and tracer) were calculated during steady-state irrigation. We irrigated the model for 50 d (13.3 mm d^{-1}; 182 L d^{-1}) until we reached hydrologic steady state, then continued irrigating at steady state for 141 d. While at steady state, daily irrigation (6.1 mm d^{-1}; 86 L d^{-1}) was similar to the mean daily average precipitation (6.5 mm d^{-1}; 89 L d^{-1}) in the wettest year on record at low

195 elevation (685 m asl) in the Coweeta Basin, and to the mean daily average at high elevation
196 (1,398 m asl; Laseter et al., 2012). The soil surface was uncovered (though the shelter remained
197 in place) during this irrigation period. We assumed evapotranspiration was negligible because
198 the model was irrigated only once daily, minimizing exposure of wet soil to the atmosphere, and
199 at 08:00, when air temperature was lower; and there was no live vegetation in the model to
200 transpire water.
201
202 At the beginning of the steady-state irrigation period we applied a conservative deuterium (^2H)
203 tracer (a mixture of 10 mL of ^2H_2O [99.9 atom % ^2H] and 90 mL of deionized water) onto the
204 model 5 m upslope from the outlet. We sampled water (Q_{out}) at the outlet to measure total
205 recovery of the mass of tracer until the ^2H signature returned to the pre-tracer background level.
206 Isotopic analysis of ^2H in Q_{out} was done on an isotopic liquid water and water vapor analyzer
207 (Model L1102-i, Picarro, Santa Clara, CA) using a modified sampling protocol and post-
208 processing correction and normalization procedures, all of which maximized precision, accuracy,
209 and efficiency (van Geldern & Barth, 2012). The precision of the method was ≤ 0.5 ‰, which
210 was within the generally accepted values (1–2 ‰) for traditional isotope ratio mass spectrometry.
211
212 ***2.1.4. Water monitoring***
213 Outflow (Q_{out}) volume was measured by a tipping bucket (500 mL increments; Snowmetrics,
214 Fort Collins, CO; Fig. 1a; Elder et al., 2014) at the outlet. Due to instrument availability, soil
215 water content was measured with two types of instruments, and one instrument type was
216 corrected to the other. Soil water content (θ) was measured at three locations (1.1, 4.9, and 8.7 m
217 upslope; 10 cm depth point increments) using capacitance-based sensors (Model Drill & Drop,

Sentek, Stepney, South Australia), and at three other locations (3.0, 6.8, and 12.5 m upslope; integrated over 30 cm depth increments) using time-domain reflectometry (TDR)-based sensors (Model CS615, Campbell Scientific, Logan, UT). A correction supplied by the manufacturer was applied to data collected from TDR-based sensors to remove bias from air and soil temperature (Campbell Scientific, 1996) and then those data were smoothed with a 24 h moving window average. Capacitance-based sensors were corrected to the TDR-based sensors during periods of soil saturation when sensor values plateaued. Saturated water contents (θ_s) were calculated as means for in situ sensor pairs (capacitance- and TDR-based sensors were paired to represent downslope, midslope, and upslope positions) in the bottom 30 cm of the soil profile at the time of initial drainage for both of our drainage experiments. Residual water contents (θ_r) were not determined in this study because the soil was not drained to a dry-enough state.

Soil water potential (expressed as pressure head [cm]) was measured by field tensiometers (Model T4, UMS, Pullman, WA) installed to 35 cm depth at three locations (0.6, 4.4, and 8.2 m upslope). A slurry of silica flour and water was placed around porous cups of tensiometers during installation to ensure good contact.

2.1.5. Drainage data analysis

Below-ground leakage from the concrete foundation of the model was estimated using the following water balance equation integrated over different time periods:

$$\Delta S = Q_{\text{in}} - Q_{\text{out}} + E + \text{Residual} \quad (1)$$

where ΔS is change in soil water storage, Q_{in} is water added, Q_{out} is outflow at the outlet pipe, and E is evaporation; the Residual term was then calculated. All units are expressed as volumes

241 (L). The ΔS, Q_{in}, and Q_{out} terms were measured and the E term was assumed to be negligible, so
242 the unaccounted for water in the Residual term was assumed to be equal to below-ground
243 leakage from the model. Terms were calculated for different specified periods (e.g., partial or
244 whole drainage, or steady-state irrigation experiment). We also calculated an overall leakage rate
245 for the drainage experiments starting from just before initiation of wetup by hand (7 [0.3 d] or 9
246 [0.4 d] hr before drainage commenced in the respective experiments) until the cessation of Q_{out}.
247 We included the period of wet-up because soil water content was stable just before wet-up, after
248 the model had been irrigated continuously at steady state; also, from wet-up to the start of
249 drainage, soil water content was highly dynamic so measurements taken in this period contained
250 some uncertainty and provided only a general estimate of leakage.
251
252 We presented drainage data in multiple ways. First, we plotted drainage curves to help
253 understand whether and how soil pedogenesis had altered bulk drainage properties of the
254 hillslope model. However, such curves showed only the outflow collected at the outlet (Q_{out}) and
255 neglected water lost to leakage, though leakage was a component of total hillslope drainage.
256 Therefore, we also plotted the change in soil moisture storage within the hillslope model, ΔS,
257 with sub-daily temporal resolution in the first 1 d of drainage and daily resolution thereafter until
258 Q_{out} ceased. Leakage rates were then estimated based on the Residual term in Eq. (1), and were
259 quantified both in terms of magnitude ($\Delta S - Q_{out}$) and proportion of total change in storage (leak
260 / ΔS).
261
262 Drainage was additionally examined by plotting the logarithms of both rates of decrease in Q_{out}
263 ($\log[\frac{-dQ_{out}}{dT}]$) and Q_{out} ($\log[Q_{out}]$). This presentation of drainage data was introduced by Brutsaert

and Nieber (1977) based on solutions to the Boussinesq equation (Boussinesq, 1904) to describe drainage deviation from an ideal, unconfined rectangular aquifer bounded by a horizontal impermeable layer, and flowing laterally into a fully penetrating stream. The theory has been applied successfully in humid, steep hillslopes, including the study hillslope for the original drainage experiment (Zecharias & Brutsaert, 1988). Short- and long-time flow regimes visually manifest themselves in the shape of the "lower envelope" of log-log plotted data, depending on the slope, b. Generally, a flow regime is categorized as short-time (b = 3), long-time (b = 3/2), or a combination of the two (b = 1; Brutsaert & Nieber, 1977). In a short-time flow regime, Q_{out} occurs shortly after wetting, and there is relatively high $\frac{-dQ_{out}}{dT}$ and Q_{out}. In principle, the largest flow rate would be observed if the entire hillslope were initially and evenly saturated, as in this study.

2.1.6. Physical and hydraulic properties of soil

Soil samples, collected before and after drainage experiments, were analyzed for physical and hydraulic properties. For analysis of physical properties, 13 intact soil cores were collected from the surface to the bottom of the model (~85 cm depth), three of which were coincident with the capacitance-based soil water content sensor locations and the remainder unrelated to instrumentation. Additionally, three intact soil cores were collected to 35 cm depth from tensiometer locations (Fig. 1a). Cores collected from instrument locations were extracted using a 2 cm diameter push-tube soil probe, and cores unrelated to instruments using a soil auger (2.2 cm diameter). The vertical profile depth from surface to concrete was estimated during soil sampling; mean depth, which was smaller than that reported in the original study, was used to calculate a new volume, mass, and bulk density for soil in the hillslope segment of the model.

We used this new volume (9.4 m^3 of soil, a decrease of 1.5 m^3 [or 14 %] across the model since the original study) and soil water content point measurements, which were linearly interpolated across the hillslope segment of the model and averaged, to estimate total volumetric water content (%) and storage (L) in the hillslope segment.

All cores were separated into 10 cm depth increments (after correcting for compaction during excavation by assuming even compaction across the lengths of the cores). Air-dried samples were further dried to 65 °C for analysis of bulk density and porosity. Subsamples were analyzed for soil texture on a particle size analyzer (Model CILAS 1190, CPS US, Fitchburg, WI) using a laser diffraction method (Konert & Vandenberghe, 1997). Other subsamples were ball-milled and analyzed for total carbon content (Model Vario MAX CNS, Elementar, Ronkonkoma, NY).

For analysis of hydraulic properties, additional cores (5.1 cm depth; 5.1 cm diameter) were collected from the surface (from 10 to 15 cm depth) layer at three locations (1.6, 7.3, and 13.0 m upslope; Fig. 1a). Soil moisture release curves were measured on a HYPROP (Meter, Pullman, WA) using the Schindler (1980) evaporation method (Peters & Durner, 2008). These soil cores were also saturated in the laboratory and used to measure saturated hydraulic conductivity (K_s) on a KSAT automated constant head device (Meter, Pullman, WA) using the falling head test method (Reynolds et al., 2002).

2.2. Numerical modeling experiments

2.2.1. Numerical model selection

Drainage and hydrologic mass balance simulations were also done using a numerical model (HYDRUS-2D, hereafter HYDRUS; Šimůnek et al., 2012). HYDRUS is a two-dimensional finite element model that simulates transport of water, heat, and solutes through variably saturated porous media by numerically solving the Richards equation for saturated-unsaturated water flow and convection-dispersion transport (Šimůnek et al., 2012). It has successfully simulated subsurface saturated and unsaturated flow through hillslopes (e.g., Hopp & McDonnell, 2009; Keim et al., 2006; Pangle et al., 2017). Hysteresis was not considered in our simulations because the physical model was wetted to near-saturation before drainage, so only the main drying portion of the water retention curve was applicable.

2.2.2. Model parameterization and calibration, and hydraulic properties of soil

The physical hillslope model was represented across a 2-D plane in numerical model space with an unstructured mesh containing 47,255 nodes that formed triangular elements. A finer resolution was used at the water table near the outlet compared with the rest of the hillslope to simulate drainage dynamics more precisely. The hillslope surface soil-air interface was represented with an "atmospheric" boundary over which irrigation water entered evenly. Concrete foundation and walls along the bottom and sides were represented with "no flux" boundaries, and the outlet through which Q_{out} left the saturated zone was represented with a "seepage face" boundary. Along this seepage face, the numerical model assumed that the pressure head was uniformly equal to zero (Šimůnek et al., 2012).

We assumed there were two soil materials in the flow domain of the numerical model. The numerical model was filled with a homogeneous sandy clay loam soil across most of the

hillslope except for a layer of pure sand just beneath the elevation of the outlet pipe at the base of the hillslope, as described in the original study (Hewlett & Hibbert, 1963). For the hillslope soil, the volumetric soil water content (θ; $cm^3\ cm^{-3}$) was estimated as a function of the water pressure head (h; cm) using the van Genuchten-Mualem model (van Genuchten, 1980):

$$\theta(h) = \theta_r + \frac{(\theta_s - \theta_r)}{[1 + (\alpha h)^n]^m} \quad (2)$$

where θ_r is the residual water content, θ_s is the saturated water content, h is positive, $m = 1 - 1/n$, and α and n are curve shape parameters. Four independent parameters (θ_r, θ_s, α, and n) were estimated using nonlinear least squares curve fitting to observed soil water retention data measured at both a nearby hillslope model that was packed with similar soil, and in our hillslope model (Table 1). The residual (θ_r) and saturated (θ_s) water contents were assumed to be 0 (Hewlett, 1961a) and 53 % (determined from Experiment 1, below), respectively. Constants α and n were estimated to be 3.44 m^{-1} and 1.25 (unitless), respectively. Saturated hydraulic conductivity (K_s) was assumed to be 8.2 cm h^{-1}, based on the results of Zacharias and Brutsaert (1988) and Steenhuis et al. (1999), and adjusted slightly during calibration. Pore-connectivity (l; unitless) was assumed to be 0.5 (Mualem, 1976). For the sand layer at the outlet, default parameters for sand in HYDRUS were used (θ_r was 5 %, θ_s was 43 %, α was 20 m^{-1}, n was 3 [unitless], and K_s was 29.7 cm h^{-1}). Pore-connectivity (l) was the same (0.5; unitless) for both the hillslope soil and sand. Model performance for simulating Q_{out} during drainage was evaluated by the Nash-Sutcliffe Efficiency (NSE; Nash & Sutcliffe, 1970).

353 In both of our physical drainage experiments, after Q_{out} ceased, we observed that pressure head at
354 the downslope tensiometer (5 cm vertically below the outlet) decreased rapidly and became
355 negative. This suggested there was persistent loss of water in the hillslope model through a
356 putative leak and that the leak was located below the elevation of this tensiometer. We repeated
357 numerical simulations of the drainage experiment with an incorporation of a leak to replicate
358 drainage curves and pressure head observations. One node (representative of 1 cm) at the joint of
359 the two concrete floors (location shown in Fig. 1b) was changed from a "no flux" to "free
360 drainage" boundary. Under free drainage, the numerical model computed a discharge rate
361 through that node according to the local value of the pressure head and the corresponding
362 hydraulic conductivity that was given for the hillslope soil adjacent to that node (Šimůnek et al.,
363 2012). By definition, the free drainage boundary condition holds the gradient in pressure head to
364 zero at a boundary (i.e., the total head gradient is equal to 1, and the flux is equal to the hydraulic
365 conductivity). Therefore, this boundary condition is appropriate (only) for the bottom of the
366 transport domain.
367
368 **3 Results**
369 **3.1. Changes in physical and hydraulic properties of soil**
370 Soil in the hillslope model experienced changes in volume, bulk density, and texture since the
371 original study (Table 1). Soil depths ranged from 71.0–87.5 and averaged 80.0 (± 2.3 SE) cm,
372 which was a decrease from 91.4 cm in the original study. Soil depths generally decreased toward
373 the lower hillslope position. Bulk densities ranged from 0.75–1.69 and averaged 1.23 (± 0.02) g
374 cm^{-3} (Fig. 2), which was a slight decrease from 1.3 g cm^{-3} in the original study. Particle size
375 analysis determined that the soil we collected was silt loam (19 % sand, 73 % silt, and 8 % clay

averaged across the hillslope; Fig. 3), though soil was originally reported to be sandy clay loam (60 % sand, 18 % silt, and 22 % clay).

There was variation with depth in soil properties, indicating horizonation. In surface layers (0–10 and 10–20 cm depth), mean bulk density was lower (0.96 ± 0.04 and 1.14 ± 0.03 g cm^{-3}, respectively; Fig. 2) than deeper in the profile (1.29 ± 0.02 g cm^{-3}). Silt proportions also varied systematically within the profile and down the slope, with mean proportion of silt being higher in surface layers (77.4 ± 0.5 % at 0–10 cm depth; 73.5 ± 0.6 % at 10–20 cm depth) than deeper in the profile (72.0 ± 0.3 %), and there was a general increase in silt lower in the hillslope (Fig. 3b). Mean organic carbon content too was higher in surface layers (1.9 ± 0.1 % at 0–10 cm depth; 0.9 ± 0.04 % at 10–20 cm depth), than deeper in the profile (0.7 ± 0.01 %). Colonization of soil by invertebrates and establishment of tree roots were observed visually at the surface, though extent of burrows and root structure were not quantified in order to limit disturbance to soil.

Despite significant changes in physical properties of soil, net changes in hydraulic properties appeared to be small. Our lab core-based measurements of soil moisture release curves were in near agreement with the original study, whereas our in situ measurements showed some deviation from the original study, due to larger water contents and concomitant higher pressure head in the in situ drainage experiments (Fig. 4). Porosity, determined by maximum soil water content at saturation (mean θ_s = 53.1 ± 0.03 %) just before drainage at multiple sensor locations, was higher than θ_s (49 %) reported for soils similar to those in the original study (Fig. 4; Hewlett, 1961a). As a reference, mean porosity, calculated from bulk density and assuming a solid phase density of 2.65 g cm^{-3}, was 53.4 (± 0.01) % across the hillslope in this study, compared to the original porosity of 50.9 %. Soil cores taken from the surface had a geometric mean K_s of 11.3 cm h^{-1} across the hillslope in this study (Table 1), which was within the range of estimates

401 previously calculated for the entire hillslope, from 8.4 (Zecharias & Brutsaert, 1988) and 8.6
402 (Steenhuis et al., 1999) to 16.8 cm h^{-1} (Sloan & Moore, 1984).
403
404 **3.2. Outflow in drainage experiments**
405 In our first drainage experiment (Experiment 1; Fig. 5), the pattern of drainage was similar to
406 that in the original experiment. Fast drainage occurred in the first 1.5 d followed by a transition
407 to slower drainage for up to ~10 d (Fig. 5a). However, unlike in the original experiment, we
408 observed a second transition point at ~10 d, when the outflow rate decreased rapidly up to the
409 cessation of Q_{out} at 17 d (Fig. 5a). During the 17 d drainage period, we estimated from the
410 difference in beginning and ending soil water storages (4,019 L at T = 0 d and 3,286 L at T = 17
411 d) that 733 L had drained from the hillslope; of this, 561 L (the sum of 435.5 [T = 0–5 d] and
412 125.5 [T = 5–17 d]) was measured exiting the outlet (Q_{out}) and 172 L were unaccounted for
413 (Residual; averaging 10 L d^{-1}; Table 2). In the original experiment, 1,260 L drained and exited
414 the outlet (Q_{out}) during a drainage period over 145 d. Most drainage occurred in the first 5 d in
415 the original and our experiments. In the first 5 d of the original experiment, 958 L were drained;
416 in comparison, in the first 5 d of our experiment, 619 L were estimated from soil water storages
417 to have drained, but only 435.5 L exited the outlet (Q_{out}), and 183.5 L were unaccounted for
418 (Residual; averaging 37 L d^{-1}).
419
420 We continued to monitor soil water content for 43 d after the cessation of Q_{out}. In the time
421 between when Q_{out} ceased (17 d) and when we terminated the experiment (60 d), mean soil water
422 content decreased from 35.1 to 33.7 % and the size of the nearly-saturated wedge diminished
423 progressively along the bottom boundary of the model at the toeslope position (Fig. 6).

Therefore, given that evaporative loss through the soil cover was negligible, the unaccounted for drainage that occurred in addition to measured Q_{out} (= 0 L) in this period suggested a leak (126 L; 3 L d^{-1}) in the lower boundary of the model. In total, from wet-up (−0.3 d) until cessation of Q_{out} (17 d), 1,500 L had been added (Q_{in}) and soil water storage was reduced by 41 L (ΔS); of this, 821 L were accounted for by outflow at the outlet (Q_{out}), and 720 L were unaccounted for (Residual), suggesting a leakage of 46.7 % of Q_{in} and at a rate of 42 L d^{-1}. The average rate of leakage in this calculation was higher than that calculated during only the drainage period (not including wet-up) due to the inclusion of high leakage during wet-up, when pressure head was highest.

In our second drainage experiment (Experiment 2), the drainage pattern was similar to our first drainage experiment and Q_{out} ceased after 12 d (Fig. 5a), confirming reproducibility of the first experiment and also further supporting possibility of a leak in the model. During this drainage period (12 d), beginning and ending soil water storages (4,080 L at T = 0 d and 3,320 L at T = 12 d) showed that 760 L were estimated to have drained from the hillslope; of this, 451 L (397.5 L at T = 0–5 d; 53.5 L at T = 5–12 d) exited the outlet (Q_{out}) and 309 L were unaccounted for (Residual; averaging 26 L d^{-1}) and possibly lost through leakage (Table 2). In the first 5 d, 685 L drained from the hillslope, but only 397.5 L exited the outlet (Q_{out}) and 287.5 L were unaccounted for (Residual; averaging 58 L d^{-1}). Again, water drained in the time after Q_{out} ceased (12 d; mean θ = 35.4 %) until the end of the experiment (48 d; mean θ = 32.8 %), suggesting a leak of 251 L (averaging 7 L d^{-1}). In total, from wetup (−0.4 d) to cessation of Q_{out} (12 d), leakage was 48.5 % of Q_{in} and at a rate of 64 L d^{-1}.

447 Calculated changes in soil moisture storage (combination of Q_{out} and leakage) were more similar
448 to the drainage curve in the original study (Fig. 7a), suggesting that pedogenesis and changes to
449 the boundary conditions had not substantially altered total soil drainage, but only Q_{out}. Leakage
450 rates were highest in the first 1 d (1,582 and 2,142 L d^{-1} in Experiments 1 and 2, respectively)
451 before decreasing nearly two orders of magnitude to 19 (Experiment 1) and 28 L d^{-1}
452 (Experiment 2; Fig. 7b), averaged from 1 d to when Q_{out} ceased (17 and 12 d, respectively). Loss
453 to leakage was the primary hydrologic output in the first 1 d, but loss to the outlet (Q_{out})
454 exceeded leakage loss between days 1 and 17 (Experiment 1; between days 1 and 12 in
455 Experiment 2), the period before Q_{out} ceased (Fig. 7c).
456
457 The numerical model (HYDRUS [no leak]) simulated Q_{out} well for the original drainage
458 experiment (Hewlett & Hibbert, 1963; NSE = 0.89; Fig. 5a) because the numerical model
459 represented the physical soil as homogeneous and isotropic, and there were no data points
460 provided by the original study for the early part of the original drainage curve ($T < 0.1$ d), when
461 macropores likely contributed to Q_{out}. The numerical model did not simulate early Q_{out} (< 0.1 d)
462 well for our Experiments 1 (NSE = 0.15) and 2 (NSE = 0.0), which included observations in the
463 early part of the drainage curve. Therefore, there was better agreement (NSE = 0.79 and 0.75 for
464 Experiments 1 and 2, respectively) when the simulation for the initial 0.1 d was excluded from
465 the model performance criterion. It was possible that a dual-domain porosity representation of
466 the hillslope would improve our results in the first 0.1 d of drainage; however, we did not have
467 enough information to parameterize the numerical model in this way. Incorporation of a leak in
468 the numerical model improved the fit between simulated (with leak) and observed drainage
469 curves (Fig. 5a) for Experiment 1 (for entire time series, NSE = 0.12; for $T > 0.1$ d, NSE = 0.84)

and 2 (for entire time series, NSE = 0.0; for time > 0.1 d, NSE = 0.81). Outflow (Q_{out}) ceased after 13.8 d in the simulation (with leak), which was similar to cessation of Q_{out} (17 and 12 d) in our physical experiments.

When Q_{out} was plotted as the logarithms of both rates of change in Q_{out} ($\log[\frac{-dQ_{out}}{dT}]$) and Q_{out} ($\log[Q_{out}]$; Fig. 5b), a break in the slope of a line enveloping the lower boundary of the data indicated a transition point between short- and long-time drainage. A similar claim about a transition point between fast and slow drainage from larger to smaller pores, respectively, after ~1.5 d of drainage was made by Hewlett and Hibbert (1963) in analyzing their drainage curve. That transition point can be seen in data from the original and our experiments approximately where lines indicating slopes of 3 and 3/2 intersect (Fig. 5b).

Drainage was similar between our experiments and the original at high and medium flows, but was different at low flows ($\log[Q_{out}] < 2$), likely due to leakage (Fig. 5b). The average slope (b = 1.77; Adj. R^2 = 0.86; $P < 0.001$) of our experiments was higher than the slope (b = 1.67; Adj. R^2 = 0.96; $P < 0.001$) for the original experiment, due to our inclusion of faster flow rates in the first 0.1 d of drainage. Slopes of our experiments were significantly different ($P < 0.001$) from the original experiment in an analysis of covariance test. When a mean slope was fit to all data from all three experiments, the average slope (b = 1.90; Adj. R^2 = 0.90; $P < 0.001$) was higher than for our experiments alone because data points at low-flows ($\log[Q_{out}]$) from the original experiment outweighed the impact of the higher values of $\log[\frac{-dQ_{out}}{dT}]$ when there was a leak.

3.3. Pressure head conditions during drainage

493 Soil water pressures head were generally similar among our drainage experiments and the
494 original experiment (Fig. 8), and corroborated Q_{out} and soil water content data. Soil water
495 pressure head was positive at the sensor located 5 cm vertically below the outlet, indicating
496 existence of a water table at nearly the same elevation as in the original experiment. Observation
497 nodes in the numerical model (with leak) at the corresponding locations of tensiometers in the
498 physical model showed similar patterns of pressure head (Fig. 8b). At the observation node
499 below the outlet, water potential became negative at the same time and decreased at similar rates
500 as in the physical experiments. However, pressure head was ~10 cm higher overall in the
501 simulation (with leak) relative to the physical experiments, both at the upslope locations (137
502 and 278 cm above the outlet) until $T \approx 1$ d and at the location below the outlet until $T \approx 3$ d. Then
503 there were lower pressure heads in the simulation (with leak) relative to the physical
504 experiments, indicating different distributions of soil water content and pressure head, both
505 spatially and temporally, in the simulation, though these differences did not appear to affect
506 simulated Q_{out}.
507
508 **3.4. Steady-state irrigation mass balance experiments**
509 When the hillslope model was irrigated at steady state, leakage was 26.1 % of water added (Q_{in})
510 when averaged over 141 d (21 L d^{-1}; Table 2). Leakage was similar (29.9 % of Q_{in}) in the
511 simulation (with leak). During this steady-state irrigation period, the mass of a conservative
512 deuterium tracer that was not recovered at the outlet in the physical model was also similar (30.0
513 % of tracer application), all of which independently corroborated presence and magnitude of a
514 leak.
515

4 Discussion

In this study we compared the flow mechanisms during drainage in an idealized hillslope model immediately after construction (Hewlett & Hibbert, 1963) and after 55 y of pedogenesis. In the time between experiments, soil complexity increased and a putative leak formed in the concrete foundation of the model, both of which rendered the model more similar to a natural forested hillslope. Our major finding was that the long, slow drainage observed in the original—and seminal—experiment did not occur in our repeat of the experiment. The drainage period was shortened due to leakage through the bottom boundary layer, analogous to realistic leakage into underlying bedrock. Observed soil changes included additions of biomass, formation of tree root networks and invertebrate burrows, soil profile development, vertical bulk density gradients, large textural changes (a shift from sand to silt), settling, and erosion, yet their resulting cumulative effect on the drainage pattern, described by rates of outflow, soil water content, and soil water pressure head, appeared to have been small relative to that imposed by the leak.

4.1. Implications of changes to soil on subsurface flow

Loss of soil volume since the original experiment was likely due to both compaction within the hillslope model, and weathering that led to particle migration through and out of the model. The deepest soil samples consistently had a higher bulk density (Fig. 2), supporting the former, and there was a higher proportion of silt relative to sand for downslope samples (Fig. 3b), supporting the latter. Further supporting the latter was that the average bulk density across the hillslope was lower in this study (1.23 [± 0.02] g cm^{-3}) relative to the original study (1.3 g cm^{-3}). We also concluded there was some mass loss because soil settling alone could not explain the observed decrease in volume.

539

540 The shift in soil texture from sandy clay loam to silt loam (Fig. 3a), combined with additions of
541 organic matter and bioturbation, possibly in turn modified the pore space in the soil matrix.
542 Aggregate formation creates macropores, and roots and invertebrates push through soil, moving
543 particles and creating large channels, all of which are favorable for preferential flow, especially
544 during initial wetting and drainage (Torres et al., 1998). Fast nonlinear flow was observed early
545 in both of our drainage curves (Fig. 5a, 7a). However, it was unclear how the fast flow rate had
546 changed since the original experiment because the monitoring system in the original experiment
547 did not incorporate data points in the first 0.1 d of drainage, when macropore flow would likely
548 dominate outflow. Though we did not observe or numerically model macropores, preferential
549 flow can occur even without presence of visually apparent macropores (Jackson et al., 2016).
550

551 Observed soil physical changes had little net effect on the soil water content and water potential
552 relationship (Fig. 4), or the general drainage pattern in the first 10 d, especially after leakage was
553 incorporated into total hillslope drainage (Fig. 5a, 7a). These results, in addition to numerical
554 simulations (Fig. 5a), support the assumption that the hillslope soil was qualitatively
555 homogenous, or at least behaved as a homogenous soil. We hypothesized that there were
556 competing hydraulic effects from multiple changes in soil properties. Reduction in dominant
557 particle size from sand to silt indicated weathering of soil, especially at the surface. This led to
558 an increase in total porosity and a likely decrease in average pore size, which should have
559 increased water retention. Less water would have been partitioned as fast flow, which moved
560 primarily due to gravity through channel networks, and more water would have been partitioned
561 as slow flow, which moved primarily due to capillary tension through the soil matrix.

562 Coincidentally, introduction of vegetation and invertebrate burrows could have also introduced
563 large pore channels that had opposing hydraulic effects. Although net differences in drainage
564 before and after pedogenesis did not appear large on a logarithmic plot, such differences, when
565 scaled up, would likely affect water resources and ecosystems, and it seems reasonable that
566 change in hydraulic properties could nevertheless be playing an important role in the movement
567 of water.
568
569 **4.2. Soil particle analyses methods**
570 The large-scale reduction in soil particle size was surprising and it was possible, though unlikely,
571 this reduction was due to an artificial discrepancy between different methods in particle size
572 analyses. Hewlett and Hibbert (1963) used a hydrometer method (Wen et al., 2002) and we used
573 a laser diffraction method (Konert & Vandenberghe, 1997). We accepted the laser diffraction
574 method as favorable for several reasons. The laser diffraction method was independent of the
575 densities of individual particles, as the calculated particle size distribution was based on
576 geometry and not mass, and reduced error from incorporating such assumptions. Also, the largest
577 change between this study and the original was in sand content, and the two methods measure
578 sand content equally well, with discrepancies primarily in the clay content (Cheetham et al.,
579 2008; Di Stefano et al., 2010; Wen et al., 2002). Furthermore, discrepancies between the two
580 methods are typically smaller mis-classifications from one textural class to an adjacent class,
581 e.g., when plotted on a soil texture triangle. Discrepancies in the literature have not been
582 observed to be large enough to change to a non-adjacent textural class (Miller & Schaetzl, 2012),
583 as they did in this study (Fig. 3a). The magnitude of change in particle size we detected was large

584 enough to overwhelm methodological differences, suggesting that there was indeed a real shift
585 from the soil being composed of mostly sand-sized particles to mostly silt-sized particles.
586
587 Such large-scale silt production in an unglaciated region is not implausible. The soil in our
588 hillslope model was excavated from the C horizon and brought up to the surface, where it may
589 have undergone relatively rapid weathering, similarly to soils elsewhere. Major conversion of
590 sand to silt due to chemical weathering has been observed in sand dunes in humid tropical
591 systems (Pye, 1983). In nearer Appalachian mine spoils of fresh unweathered parent material
592 (mixed sandstone and siltstone), there were also large conversions of sand to silt that occurred
593 quickly (<2 y) after excavation, exposure to a humid surface environment, and incorporation of
594 organic matter (fertilizer and seeds) across the surface (Roberts et al., 1988). There, biological
595 processing occurred, which led to dissolution, leaching, and oxidation of soil. Also there, water
596 retention increased slightly (as in this study) as a result of changes in soil texture and organic
597 matter addition.
598
599 **4.3. Implications of a leaky soil boundary condition to baseflow**
600 In the original drainage experiment (Hewlett & Hibbert, 1963) the hillslope model continued
601 draining long after piezometers at the base of the model showed unsaturated conditions in the
602 entirety of the hillslope (~2–3 days), leading to the explanation that unsaturated flow continued
603 to feed the saturated area at the outlet. The plastic covering and concrete floor created no-flow
604 boundary conditions such that downslope was the only direction unsaturated water could drain.
605 Zaslavsky and Sinai's (1981) Richards's equation model shows how such boundary conditions
606 can force unsaturated lateral downslope flow. The resulting drainage curve (i.e., Q_{out} over time)

607 presented by Hewlett and Hibbert (1963) was highly influential in understanding physical and
608 hydraulic properties of a hillslope.
609
610 However, other work in a similar, but scaled-down, physical model has shown that spurious
611 inferences about physical processes can be drawn from such graphical analysis of drainage
612 curves because the curves present break points that possibly do not have physical meaning
613 (Anderson & Burt, 1977; Anderson & Burt, 1980). Therefore, the rate of progressive diminution
614 of the geometric dimensions of the saturated wedge (which may not include such break points),
615 rather than the mathematical relationship between Q_{out} and time, has been argued to be a better
616 predictor of Q_{out}. Our drainage experiments supported the assertion that long-term drainage
617 cannot be fully accounted for without considering the constant contribution of water from
618 unsaturated soil upslope to the saturated wedge (Fig. 6). However, a focus on only the
619 diminution of the saturated wedge can lead to incorrect conclusions about timing and volume of
620 Q_{out} at the outlet if water is siphoned off through a leak, as happened in this study.
621
622 The leak in our model was analogous to a realistic leak to bedrock fractures commonly found in
623 many natural catchments, and also may occur as groundwater discharge features (e.g., Iwagami
624 et al., 2010; Montgomery et al., 1997). The magnitude (26 % of Q_{in}; Table 2) of the leak in our
625 steady-state irrigation experiment was within the range of water loss from the soil mantle to
626 bedrock in two small Japanese catchments (18 and 30 % of precipitation; Terajima et al., 1993).
627 The leak (47–49 % of Q_{in}) in our drainage experiments was larger and within the range of
628 leakage elsewhere, which ranges from 35 to 55 % of precipitation at a small headwater
629 catchment in the Kiryu Experimental Watershed in Japan (Kosugi et al., 2006) to 41 % at the M8

630 catchment near the Maimai experimental hillslope in New Zealand (Graham et al., 2010) to 44 %
631 at ephemeral headwater catchments in Idaho, USA (Aishlin & McNamara, 2011). Leaks have
632 been even larger elsewhere, from 66 % across high-mountain catchments in Wyoming, USA
633 (Flinchum et al., 2018), to 91 % at a trenched experimental hillslope at the Panola Mountain
634 Research Watershed in Georgia, USA (Tromp-van Meerveld et al., 2007). At Coweeta, long
635 flowpaths through fractured bedrock have been suspected to delay hydrologic responses over
636 many months or even years (Post & Jones, 2001).
637
638 Many studies have shown that microtopography and permeability of bedrock, rather than the soil
639 surface, can be key variables to timing and volume of runoff (Freer et al., 2002; Graham et al.,
640 2010; Hopp & McDonnell, 2009; Lehmann et al., 2007; McGlynn & McDonnell, 2003; Salve et
641 al., 2012; Tani, 1997; Tromp-van Meerveld & McDonnell, 2006). This study elucidates further
642 the impacts of size and location of a leak on timing and volume of drainage from hillslope soils.
643 In our numerical model, only a small leak (representative of 1 cm width) was required to
644 decrease the drainage period by nearly an order of magnitude, from 145 d in the original
645 experiment to ~14 d (Fig. 5a). In preliminary numerical model runs, a leak of the same size but
646 placed at a different location (6 m upslope along the lower boundary) had a negligible impact on
647 the shape of the drainage curve due to the smaller pressure head. This suggested analogous
648 bedrock fractures in the riparian zone can disconnect the hillslope from the outlet and largely
649 impact timing of water and solute movement to the stream.
650
651 We used the same hillslope model and experimental design of the original and highly influential
652 study whose results (along with a precursor study [Hewlett 1961a]) led to the development of the

653 VSA concept (formalized in Hewlett & Hibbert 1967), an important paradigm in hillslope
654 hydrology, and we showed that leakage from surface soil should be considered in future studies
655 of soil drainage to streams. A leakage term in our study did not invalidate the VSA concept, but
656 rather provided further support for it. The original experiment showed, through the VSA concept,
657 that areas contributing water would contract in the recession period and cause nonlinear
658 contributions from shallow soil to baseflow for a long time (Hewlett & Hibbert, 1963). Our
659 experiments showed that flow along the hillslope is still connected to the stream, though, in a
660 more natural hillslope, the direct contribution from surface soil can be much smaller than
661 previously thought (Fig. 5a), and the indirect contribution, which is rerouted through cracks and
662 fractures in bedrock, can be much larger, as observed elsewhere (Graham et al., 2010; Salve et
663 al., 2012). This rerouting of water can further increase the variability and nonlinearity of long,
664 slow drainage during the recession period, as the VSA concept suggests.
665
666 This study also showed that a hillslope surface soil that has experienced soil pedogenic
667 processing and leaks can still move water quickly to the outlet with little impact to the beginning
668 of the drainage curve (Fig. 5a). Our drainage curves did not deviate from the original curve until
669 12–17 d after initiation of drainage, so the impact of a leak on timing and volume of drainage
670 would be larger between irrigation (and precipitation) events than during an event. Drought
671 severity and frequency have increased at Coweeta (Laseter et al., 2012), in the United States
672 (Strzepek et al., 2010), and around the world (Vicente-Serrano et al., 2014; Yu et al., 2014) due
673 to more extreme variation in the distribution of precipitation throughout the year. Forecasted
674 periods of increased drought could severely delay hillslope contributions to baseflow where
675 leaky bedrock flow has been observed to be a significant term in the water balance. Some

676 catchments may be less resilient, with lower potential to store water in soils over long periods
677 and release water gradually (Carey et al., 2010), than previously thought.
678
679 **5 Conclusion**
680 The Hewlett (1961a) and Hewlett and Hibbert (1963) experiments have led hydrologists to
681 believe that lateral downslope unsaturated flow in mountain environments can sustain stream
682 baseflows for long periods. We hypothesized that 55 years of tree growth, litter deposition and
683 decomposition, aggregate formation, invertebrate burrowing, weathering, erosion, and associated
684 pedogenic processes would substantially alter drainage from Hewlett and Hibbert's (1963)
685 inclined hillslope soil model. Soil sampling and analyses revealed development of a thin A
686 horizon, stratification of bulk densities, downslope gradation of silt fractions, and accumulation
687 of soil carbon. Lab measurements of moisture release curves and K_s values, however, indicated
688 little change in soil hydraulic properties. Two repetitions of the Hewlett and Hibbert (1963)
689 drainage experiment revealed no changes in the recession drainage curve for the period between
690 0.1 and 10 days. Two-dimensional numerical modeling informed by empirically-derived soil
691 hydraulic parameters also did not predict a change in drainage. These experiments raise
692 questions about how much pedogenesis is required to induce significant changes in lateral
693 subsurface flow behavior.
694
695 In our drainage experiments, the long, slow drainage could not be reproduced. Creation of
696 leakage in the bottom of the model, analogous to soil recharge into bedrock fractures, had the
697 largest impact to the duration of drainage, reducing it by nearly an order of magnitude in our
698 experiments compared to the original, but with little impact to the shape of the rest of the

699 drainage curve. This suggests that leakage to bedrock, which is common in many natural
700 hillslopes, could have large impacts on recession drainage, particularly in between precipitation
701 events, rather than immediately after an event. What our experiments showed is that the long-
702 accepted explanation of mountain stream hydrology given by Hewlett and Hibbert (1963) does
703 not apply to the same degree under conditions where the bedrock is not impervious. If leakage is
704 considered in hillslopes, we see that bedrock water in addition to unsaturated drainage from
705 hillslopes has to become a significant component of baseflow maintenance. The fact that
706 hydraulic behavior of the soil matrix did not vary between our and the original experiments was
707 surprising and motivates more work on the rate of hydrologic recovery from soil disturbance or
708 land use change.
709
710 **Acknowledgements**
711 This research was supported, in part, by the Virginia Agricultural Experiment Station and the
712 McIntire-Stennis Program of the National Institute of Food and Agriculture at the U.S.
713 Department of Agriculture. Additionally, this research was supported by grants from the Virginia
714 Water Resources and Research Center, the Edna Bailey Sussman Foundation, the USDA Forest
715 Service, Coweeta Hydrologic Lab project funds, and the Institute for Critical Technology and
716 Applied Science at Virginia Tech. The authors are grateful to the staff at Coweeta Hydrologic
717 Laboratory for their assistance and hospitality while in the field. Finally, the authors are grateful
718 to three anonymous reviewers for their time and effort to offer suggestions, which significantly
719 improved the manuscript. The outflow data for drainage experiments (Hewlett & Hibbert, 1963,
720 and this study [in situ and numerically modeled]) are available at
721 https://portal.edirepository.org/nis/mapbrowse?scope=knb-lter-cwt&identifier=5023

722 and https://data.lib.vt.edu/files/hh63sv983.

723

724 **Figure Captions:**

725 **Figure 1. (a)** Top view of the hillslope soil model with locations of monitoring instruments, soil
726 core samples, and trees that were cut down and removed. Symbols indicating trees show their
727 relative sizes. There is a horizontal exaggeration of 2. **(b)** Side view of the model with moisture
728 sensors, tensiometers, and trees (hillslope positions). The black circle with saltire indicates the
729 location of the leak added to select modeling runs in the numerical model. There is no horizontal
730 exaggeration and zero on the vertical axis corresponds to the base of the model.

731

732 **Figure 2.** Bulk density profiles along the hillslope. The mean in this study is shown with a red
733 line and the uniform bulk density (1.3 g cm^{-3}) reported in the original study is shown with a
734 dashed line.

735

736 **Figure 3. (a)** Soil textural class in this study (silt loam) and reported in the original study (sandy
737 clay loam) plotted on a USDA soil texture triangle. **(b)** Percent sand versus percent silt
738 throughout the depth profile and across the hillslope.

739

740 **Figure 4.** Soil moisture release curves using field data at a similar hillslope soil model (Hewlett,
741 1961); paired soil water potential and soil water content data in the study hillslope (1.1 [down],
742 4.9 [mid], and 8.7 [up] m upslope; all 35 cm depth) for our first drainage experiment; and data
743 from saturation experiments done in the lab to soil cores taken from the study hillslope (7.3
744 [mid], and 13 [up] m upslope; all 15 cm depth). Additional points (squares) placed on the x-axis

745 show values of maximum soil water content for sensors that were saturated as determined with a
746 paired tensiometer.
747
748 **Figure 5. (a)** Time series of outflow (Q_{out}; L d^{-1}) observed and numerically simulated
749 (HYDRUS) in this study compared to results from the original experiment (Hewlett & Hibbert,
750 1963). **(b)** Log transformed Q_{out} data (log[Q_{out} (L d^{-1})] and log[$\frac{-dQ_{out}}{dT}$ (L d^{-2})]) in this study
751 compared to results from the original experiment. The average slope (b = 1.77) of experiments in
752 this study was only slightly higher than the slope (b = 1.67) for the original experiment, and the
753 average slope of all three experiments (b = 1.90) was higher than the current and original
754 experiments. Lines indicate a top envelope (slope b = 1), two bottom envelopes (slopes b = 3/2
755 and b = 3), and maximum Q_{out}.
756
757 **Figure 6.** Linearly interpolated volumetric soil water content, θ, at 0, 2, 10, 20, and 60 d after
758 drainage was initiated for our first drainage experiment (Experiment 1). Circles indicate
759 locations of moisture sensors. There is no horizontal exaggeration.
760
761 **Figure 7. (a)** Time series of total loss in hillslope water storage, ΔS (L d^{-1}; solid colored lines),
762 which we assumed to be equal to the sum of Q_{out} and leakage, and Q_{out} only observed in this
763 study (dashed colored lines), observed in the original experiment (Hewlett & Hibbert, 1963;
764 circles), and simulated numerically (HYDRUS; solid grey line). **(b)** Time series of the leak as a
765 volumetric rate ($\Delta S - Q_{out}$; L d^{-1}). Leakage rate estimated during our steady-state irrigation
766 experiment is also shown. **(c)** Time series of leakage as an instantaneous relative proportion of

767 total change in storage (leakage / ΔS; %). Leakage estimated during steady-state irrigation is also
768 shown.
769
770 **Figure 8. (a)** Time series of pressure head (cm) at different elevations relative to the outlet in our
771 physical experiments compared to results from the original experiment (Hewlett & Hibbert
772 1963). There were sensors at three elevations in this study and at four in the original experiment.
773 **(b)** Time series of pressure head (cm) at different elevations relative to the outlet observed in our
774 physical experiments compared to in numerical simulations (with leak). Observed and
775 numerically simulated pressure head correspond to the same elevations. Points (circles) on the x-
776 axis show the times when Q_{out} ceased in each experiment.

References

Aishlin, P., & McNamara, J. P. (2011). Bedrock infiltration and mountain block recharge accounting using chloride mass balance. *Hydrological Processes*, *25*(12), 1934–1948.

Ambroise, B. (2004). Variable 'active' versus 'contributing' areas or period: a necessary distinction. *Hydrological Processes*, *18*(6), 1149–1155.

Ameli, A. A., Amvrosiadi, N., Grabs, T., Laudon, H., Creed, I. F., McDonnell, J. J., & Bishop, K. (2016). Hillslope permeability architecture controls on subsurface transit time distribution and flow paths. *Journal of Hydrology*, *543*, 17–30.

Anderson, M. G., & Burt, T. P. (1977). A laboratory model to investigate the soil moisture conditions on a draining slope. *Journal of Hydrology*, *33*, 383–390.

Anderson, M. G., & Burt, T. P. (1980). Interpretation of recession flow. *Journal of Hydrology*, *46*, 89–101.

Ankenbauer, K., & Loheide, S. P. (2016). The effects of soil organic matter on soil water retention and plant water use in a meadow of the Sierra Nevada, CA. *Hydrological Processes*, *31*(4), 891–901.

Appels, W. M., Graham, C. B., Freer, J. E., & McDonnell, J. J. (2015). Factors affecting the spatial pattern of bedrock groundwater recharge at the hillslope scale. *Hydrological Processes*, *29*(21), 4594–4610.

Bernier, P. Y. (1985). Variable source areas and storm-flow generation: an update of the concept and a simulation effort. *Journal of Hydrology*, *79*, 195–213.

Beven, K. (1982). On subsurface stormflow: An analysis of response times. *Hydrological Sciences Journal*, *27*(4), 505–521.

Beven, K., & Germann, P. (1982). Macropores and water flow in soils. *Water Resources Research*, *18*(5), 1311–1325.

Beven, K. J., & Kirkby, M. J. (1979). A physically based, variable contributing area model of basin hydrology / Un modèle à base physique de zone d'appel variable de l'hydrologie du bassin versant. *Hydrological Sciences Journal*, *24*(1), 43–69.

Bonell, M. (1998). Selected challenges in runoff generation research in forests from the hillslope to headwater drainage basin scale. *Journal of the American Water Resources Association*, *34*(4), 765–785.

Boussinesq, J. (1904). Recherches théoriques sur l'écoulement des nappes d'eau infiltrées dans le sol et sur le debit des sources. *Journal de Mathématiques Pures et*

823 *Appliquées*, *10*, 5–78.
824
825 Brutsaert, W., & Nieber, J. L. (1977). Regionalized drought flow hydrographs from a
826 mature glaciated plateau. *Water Resources Research*, *13*(3), 637–643.
827
828 Campbell Scientific. (1996). Instruction manual. CS615 Water Content Reflectometer.
829 Logan, UT: Campbell Scientific.
830
831 Carey, S. K., Tetzlaff, D., Seibert, J., Soulsby, C., Buttle, J., Laudon, H., et al. (2010).
832 Inter-comparison of hydro-climatic regimes across northern catchments:
833 synchronicity, resistance and resilience. *Hydrological Processes*, *24*(24), 3591–
834 3602.
835
836 Cheetham, M. D., Keene, A. F., Bush, R. T., Sullivan, L. A., & Erskine, W. D. (2008). A
837 comparison of grain-size analysis methods for sand-dominated fluvial sediments.
838 *Sedimentology*, *55*(6), 1905–1913.
839
840 Chorley, R. J. (1978). Glossary of Terms. In M. J. Kirkby (Ed.), *Hillslope Hydrology* (pp.
841 365–375). Chichester, U.K.: John Wiley & Sons, Inc.
842
843 Clothier, B. E., Green, S. R., & Deurer, M. (2008). Preferential flow and transport in soil:
844 progress and prognosis. *European Journal of Soil Science*, *59*(1), 2–13.
845
846 Di Stefano, C., Ferro, V., & Mirabile, S. (2010). Comparison between grain-size analyses
847 using laser diffraction and sedimentation methods. *Biosystems Engineering*,
848 *106*(2), 205–215.
849
850 Dunne, T. (1983). Relation of field studies and modeling in the prediction of storm
851 runoff. *Journal of Hydrology*, *65*, 25–48.
852
853 Elder, K, Marshall, H. P., Elder, L., Starr, B., Karlson, A., & Robertson, J. (2014).
854 *Design and installation of a tipping bucket snow lysimeter*. Paper presented at
855 International Snow Science Workshop, Banff, Canada.
856
857 Elsenbeer, H. (2001). Hydrologic flowpaths in tropical rainforest soilscapes—a
858 review. *Hydrological Processes*, *15*(10), 1751–1759.
859
860 Flinchum, B. A., Holbrook, W. S., Grana, D., Parsekian, A. D., Carr, B. J., Hayes, J. L.,
861 & Jiao, J. (2018). Estimating the water holding capacity of the critical zone using
862 near-surface geophysics. *Hydrological Processes*, *32*(22), 3308–3326.
863
864 Frankenberger, J. R., Brooks, E. S., Walter, M. T., Walter, M. F., & Steenhuis, T. S.
865 (1999). A GIS-based variable source area hydrology model. *Hydrological*
866 *Processes*, *13*(6), 805–822.
867
868 Freer, J., McDonnell, J. J., Beven, K. J., Peters, N. E., Burns, D. A., Hooper, R. P., et al.

(2002). The role of bedrock topography on subsurface storm flow. *Water Resources Research*, *38*(12), 1269. https://doi.org/10.1029/2001WR000872

Gabrielli, C. P., Morgenstern, U., Stewart, M. K., & McDonnell, J. J. (2018). Contrasting groundwater and streamflow ages at the Maimai Watershed. *Water Resources Research*, *54*(6), 3937–3957.

Genereux, D. P., & Hemond, H. F. (1990). Three-component tracer model for stormflow on a small Appalachian forested catchment—comment. *Journal of Hydrology*, *117*, 377–380.

Golden, H. E., Lane, C. R., Amaty, D. M., Bandilla, K. W., Kiperwas, H. R., Knightes, C. D., & Ssegane, H. (2014). Hydrologic connectivity between geographically isolated wetlands and surface water systems: A review of select modeling methods. *Environmental Modelling and Software*, *53*, 190–206.

Graham, C. B., Woods, R. A., & McDonnell, J. J. (2010). Hillslope threshold response to rainfall: (1) A field based forensic approach. *Journal of Hydrology*, *393*, 65–76.

Hale, V. C., & McDonnell, J. J. (2016). Effect of bedrock permeability on stream base flow mean transit time scaling relations: 1. A multiscale catchment intercomparison. *Water Resources Research*, *52*(2), 1358–1374.

Harr, R. D. (1977). Water flux in soil and subsoil on a steep forested slope. *Journal of Hydrology*, *33*, 37–58.

Hendrickx, J. M. H., & Flurry, M. (2001). Uniform and preferential flow mechanisms in the vadose zone. In National Research Council (Eds.), *Conceptual Models of Flow and Transport in the Fractured Vadose Zone* (pp. 163–209). Washington, DC: National Academies Press.

Hewlett, J. D. (1961a). Soil moisture as a source of base flow from steep mountain watersheds. In *Southeastern Forest Experiment Station Paper 132* (pp. 1–11). Asheville, NC: U.S. Forest Service.

Hewlett, J. D. (1961b). Watershed management. In *Report for 1961 Southeastern Forest Experimental Station* (pp. 61–66). Asheville, NC: U.S. Forest Service.

Hewlett, J. D., & Hibbert, A. R. (1963). Moisture and energy conditions within a sloping soil mass during drainage. *Journal of Geophysical Research*, *68*(4), 1081–1087.

Hewlett, J. D., & Hibbert, A. R. (1967). Factors affecting the response of small watersheds to precipitation in humid areas. In W. E. Sopper & H. W. Lull (Eds.), *Forest Hydrology* (pp. 275–290). New York, NY: Pergamon Press.

Hopp, L., & McDonnell, J. J. (2009). Connectivity at the hillslope scale: identifying

interactions between storm size, bedrock permeability, slope angle and soil depth. *Journal of Hydrology*, *376*, 378–391.

Iwagami, S., Tsujimura, M., Onda, Y., Shimada, J., & Tanaka, T. (2010). Role of bedrock groundwater in the rainfall-runoff process in a small headwater catchment underlain by volcanic rock. *Hydrological Processes*, *24*(19), 2771–2783.

Jackson, C. R., Du, E., Klaus, J., Griffiths, N. A., Bitew, M., & McDonnell, J. J. (2016). Interactions among hydraulic conductivity distributions, subsurface topography, and transport thresholds revealed by a multitracer hillslope irrigation experiment. *Water Resources Research*, *52*(8), 6186–6206.

Keim, R. F., Tromp-van Meerveld, H. J., & McDonnell, J. J. (2006). A virtual experiment on the effects of evaporation and intensity smoothing by canopy interception on subsurface stormflow generation. *Journal of Hydrology*, *327*, 352–364.

Kirkby, M. (1988). Hillslope runoff processes and models. *Journal of Hydrology*, *100*, 315–339.

Klaus, J., & Jackson, C. R. (2018). Interflow is not binary: A continuous shallow perched layer does not imply continuous connectivity. *Water Resources Research*, *54*(9), 5921–5932.

Konert, M., & Vandenberghe, J. (1977). Comparison of laser grain size analysis with pipette and sieve analysis: a solution for the underestimation of the clay fraction. *Sedimentology*, *44*(3), 523–535.

Kosugi, K., Katsura, S., Katsuyama, M., & Mizuyama, T. (2006). Water flow processes in weathered granitic bedrock and their effects on runoff generation in a small headwater catchment. *Water Resources Research*, *42*(2), W02414. https://doi.org/10.1029/2005WR004275

Laseter, S. H., Ford, C. R., Vose, J. M., & Swift, L. W., Jr. (2012). Long-term temperature and precipitation trends at the Coweeta Hydrologic Laboratory, Otto, North Carolina, USA. *Hydrology Research*, *43*(6), 890–901.

Lehmann, P., Hinz, C., McGrath, G., Tromp-van Meerveld, H. J., & McDonnell, J. J. (2007). Rainfall threshold for hillslope outflow: an emergent property of flow pathway connectivity. *Hydrology and Earth System Sciences*, *11*, 1047–1063.

Lyon, S. W., Walter, M. T., Gérard-Marchant, P., & Steenhuis, T. S. (2004). Using a topographic index to distribute variable source area runoff predicted with the SCS curve-number equation. *Hydrological Processes*, *18*(15), 2757–2771.

McGlynn, B. L., & McDonnell, J. J. (2003). Quantifying the relative contributions of riparian and hillslope zones to catchment runoff. *Water Resources Research*, *39*(11), 1310. https://doi.org/10.1029/2003WR002091

McGuire, K. J., & McDonnell, J. J. (2010). Hydrological connectivity of hillslopes and streams: characteristic time scales and nonlinearities. *Water Resources Research*, *46*(10), W10543. https://doi.org/10/1029/2010WR009341

Miller, B. A., & Schaetzl, R. J. (2012). Precision of soil particle size analysis using laser diffractometry. *Soil Science Society of America Journal*, *76*, 1719–1727.

Montgomery, D. R., Dietrich, W. E., Torres, R., Anderson, S. P., Heffner, J. T., & Loague, K. (1997). Hydrologic response of a steep, unchanneled valley to natural and applied rainfall. *Water Resources Research*, *33*(1), 91–109.

Moore, R. D. (1997). Storage-outflow modeling of streamflow recessions, with application to a shallow-soil forested catchment. *Journal of Hydrology*, *198*, 260–270.

Mosley, M. P. (1979). Streamflow generation in a forested watershed, New Zealand. *Water Resources Research*, *15*(4), 795–806.

Mualem, Y. (1976). A new model for predicting the hydraulic conductivity of unsaturated porous media. *Water Resources Research*, *12*(3), 513–522.

Nash, J. E., & Sutcliffe, J. V. (1970). River flow forecasting through conceptual models, Part 1—A discussion of principles. *Journal of Hydrology*, *10*, 282–290.

Nippgen, F., McGlynn, B. L., & Emanuel, R. E. (2015). The spatial and temporal evolution of contributing areas. *Water Resources Research*, *51*(6), 4550–4573.

Pangle, L. A., Kim, M., Cardoso, C., Lora, M., Neto, A. A. M., Volkmann, T. H. M., et al. (2017). The mechanistic basis for storage-dependent age distributions of water discharged from an experimental hillslope. *Water Resources Research*, *53*(4), 2733–2754.

Peters, A., & Durner, W. (2008). Simplified evaporation method for determining soil hydraulic properties. *Journal of Hydrology*, *356*, 147–162.

Pfister, L., Martínez-Carreras, N., Hissler, C., Klaus, J., Carrer, G. E., Stewart, M. K., & McDonnell, J. J. (2017). Bedrock geology controls on catchment storage, mixing, and release: a comparative analysis of 16 nested catchments. *Hydrological Processes*, *31*(10), 1828–1845.

Post, D. A., & Jones, J. A. (2001). Hydrologic regimes of forested, mountainous, headwater basins in New Hampshire, North Carolina, Oregon, and Puerto Rico.

Advances in Water Resources, *24*, 1195–1210.

Pye, K. (1983). Formation of quartz silt during humid tropical weathering of dune sands. *Sedimentary Geology*, *34*(4), 267–282.

Reynolds, W. D., Elrick, D. E., Youngs, E. G., H. Booltink, W. G., & Bouma, J. (2002). Saturated and field saturated water flow parameters: Laboratory methods. In J. H. Dane & J. W. Hopmans (Eds.), *Methods of Soil Analysis Part 4, Physical Methods, SSSA Book Series, Vol. 5* (pp. 688–690). Madison, WI: Soil Science Society of America.

Richards, L. A. (1931). Capillary conduction of liquids through porous mediums. *Physics, 1*(5): 318–333.

Roberts, J. A., Daniels, W. L., Bell, J. C., & Berger, J. A. (1988). Early stages of mine soil genesis in a southwest Virginia spoil lithosequence. *Soil Science Society of America Journal, 52*(3), 716–723.

Rothacher, J. (1965). Streamflow from small watersheds on the western flope of the Cascade Range of Oregon. *Water Resources Research*, *1*(1), 125–134.

Salve, R., Rempe, D. M., & Dietrich, W. E. (2012). Rain, rock moisture dynamics, and the rapid response of perched groundwater in weathered, fractured argillite underlying a steep hillslope. *Water Resources Research*, *48*(11), W11528. https://doi.org/10.1029/2012WR012583

Schindler, U. (1980). Ein schnellverfahren zur messung der wasserleitfähigkeit im teilgesättigten boden an stechzylinderproben. *Archiv für Acker- und Pflanzenbau und Bodenkunde*, *24*, 1–7.

Scholl, D. G., & Hibbert, A. R. (1973). Unsaturated flow properties used to predict outflow and evapotranspiration from a sloping lysimeter. *Water Resources Research*, *9*(6), 1645–1655.

Šimůnek, J., Van Genuchten, M. T., & Šejna, M. (2012). The HYDRUS software package for simulating two- and three-dimensional movement of water, heat, and multiple solutes in variably-saturated porous media, version 2.0. (Tech. Manual, pp. 230). Prague, Czech Republic: PC-Progress.

Soil Survey Staff, Natural Resources Conservation Service, United States Department of Agriculture. (2019). Official Soil Series Descriptions. Available online. Accessed 01/21/2019.

Sloan, P. G., & Moore, I. D. (1984). Modeling subsurface stormflow on steeply sloping forested watersheds. *Water Resources Research, 20*(12), 1815–1822.

Stagnitti, F., Parlange, M. B., Steenhuis, T. S., & Parlange, J.-Y. (1986). Drainage from a uniform soil layer on a hillslope. *Water Resources Research*, *22*(5), 631–634.

Steenhuis, T. S., Parlange, J.-Y., Sanford, W. E., Heilig, A., Stagnitti F., & Walter, M. F. (1999). Can we distinguish Richards' and Boussinesq's equations for hillslopes?: the Coweeta experiment revisited. *Water Resources Research*, *35*(2), 589–593.

Strzepek, K., Yohe, G., Neumann, J., & Boehlert, B. (2010). Characterizing changes in drought risk for the United States from climate change. *Environmental Research Letters*, *5*(4), 044012. https://doi.org/10.1088/1748-9326/5/4/044012

Tani, M. (1997). Runoff generation processes estimated from hydrological observations on a steep forested hillslope with a thin soil layer. *Journal of Hydrology*, *200*, 84–109.

Terajima T., Mori, A., & Ishii, H. (1993). Comparative study of deep percolation amount in two small catchments in granitic mountain. *Japanese Journal of Hydrological Sciences*, *23*, 105–118.

Torres, R., Dietrich, W. E., Montgomery, D. R., Anderson, S. P., & Loague, K. (1998). Unsaturated zone processes and the hydrologic response of a steep, unchanneled catchment. *Water Resources Research*, *34*(8), 1865–1879.

Tromp-van Meerveld, H. J., & McDonnell, J. J. (2006). Threshold relations in subsurface stormflow: 2. The fill and spill hypothesis. *Water Resources Research*, *42*(2), W02411. https://doi.org/10.1029/2004WR003800

Tromp-van Meerveld, H. J., Peters, N. E., & McDonnell J. J. (2007). Effect of bedrock permeability on subsurface stormflow and the water balance of a trenched hillslope at the Panola Mountain Research Watershed, Georgia, USA. *Hydrological Processes*, *21*(6), 750–769.

van Geldern, R., & Barth, J. A. C. (2012). Optimization of instrument setup and post-run corrections for oxygen and hydrogen stable isotope measurements of water by isotope ratio infrared spectroscopy (IRIS). *Limnology and Oceanography: Methods*, *10*(12), 1024–1036.

van Genuchten, M. T. (1980). A closed-form equation for predicting the hydraulic conductivity of unsaturated soils. *Soil Science Society of America Journal*, *44*(5), 892–898.

Vicente-Serrano, S. M., Lopez-Moreno, J.-I., Beguería, S., Lorenzo-Lacruz, J., Sanchez-Lorenzo, A., García-Ruiz, J. M., et al. (2014). Evidence of increasing drought severity caused by temperature rise in southern Europe. *Environmental Research Letters*, *9*(4), 044001. https://doi.org/10.1088/1748-9326/9/4/044001

Ward, R. C. (1984). On the response to precipitation of headwater streams in humid areas. *Journal of Hydrology*, *74*, 171–189.

Weiler, M., McDonnell, J. J., Tromp-van Meerveld, I., & Uchida, T. (2005). Subsurface stormflow. In M. G. Anderson & J. J. McDonnell (Eds.), *Encyclopedia of Hydrological Sciences* (pp. 1719–1732). John Wiley & Sons, Inc.

Wen, B., Aydin, A., & Duzgoren-Aydin, N. S. (2002). A comparative study of particle size analyses by sieve-hydrometer and laser diffraction methods. *Geotechnical Testing Journal*, *25*(4), 434–442.

Weyman, D. R. (1973). Measurements of the downslope flow of water in a soil. *Journal of Hydrology*, *20*, 267–288.

Whipkey, R. Z. (1965). Subsurface stormflow from forested slopes. *Hydrological Sciences Journal*, *10*(2), 74–85.

Wolock, D. M., & McCabe, G. J., Jr. (1995). Comparison of single and multiple flow direction algorithms for computing topographic parameters in TOPMODEL. *Water Resources Research*, *31*(5), 1315–1324.

Yu, M., Li, Q., Hayes, M. J., Svoboda, M. D., & Heim, R. R. (2014). Are droughts becoming more frequent or severe in China based on the Standardized Precipitation Evapotranspiration Index: 1951–2010? *International Journal of Climatology*, *34*(3), 545–558.

Zaslavsky, D., & Rogowski, A. S. (1969). Hydrologic and morphologic implications of anisotropy and infiltration in soil profile development. *Soil Science Society of America Proceedings*, *33*, 594–599.

Zaslavsky, D., & Sinai, G. (1981). Surface hydrology: IV—Flow in sloping, layered soil. *Journal of the Hydraulics Division*, *107*(1), 53–64.

Zecharias, Y.B., & Brutsaert, W. (1988). Recession characteristics of groundwater outflow and baseflow from mountainous watersheds. *Water Resources Research, 24*(10), 1651–1658.

Figure1.

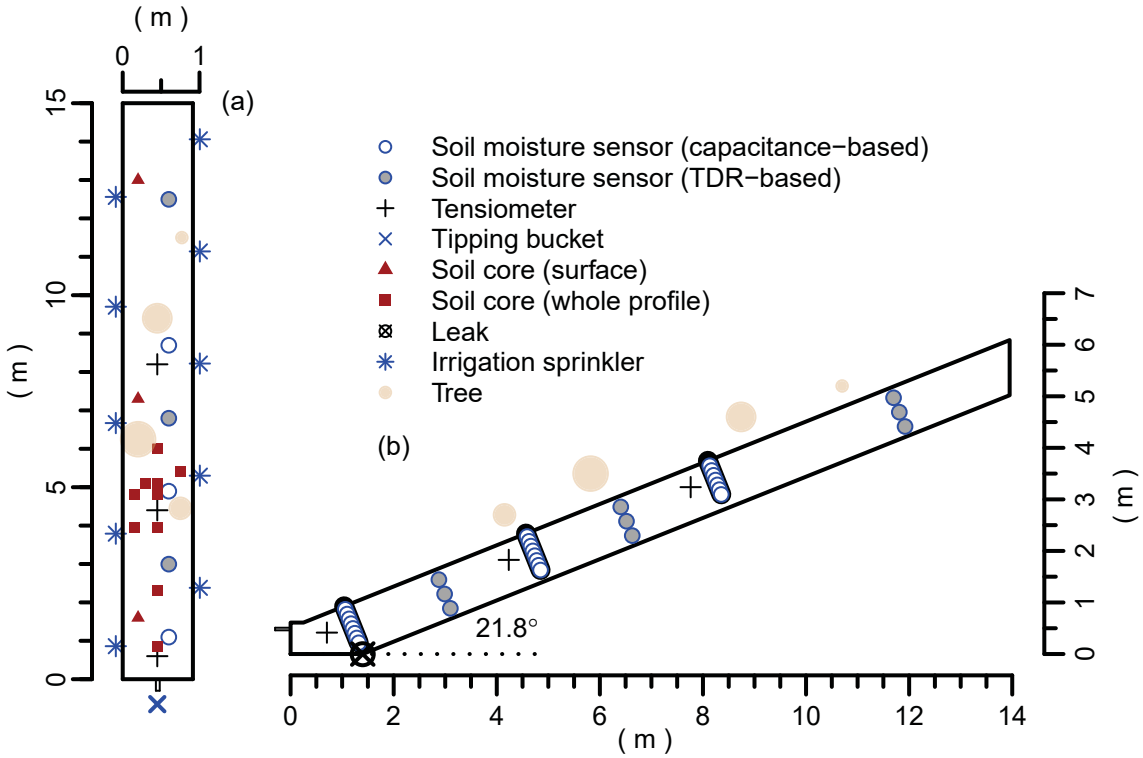
(m)
0
1
(a)
15
10
5
0
(m)
Soil moisture sensor (capacitance−based)
Soil moisture sensor (TDR−based)
Tensiometer
Tipping bucket
Soil core (surface)
Soil core (whole profile)
Leak
Irrigation sprinkler
Tree
(b)
21.8°
0
2
4
6
8
10
12
14
(m)
0
1
2
3
4
5
6
7
(m)

Figure2.

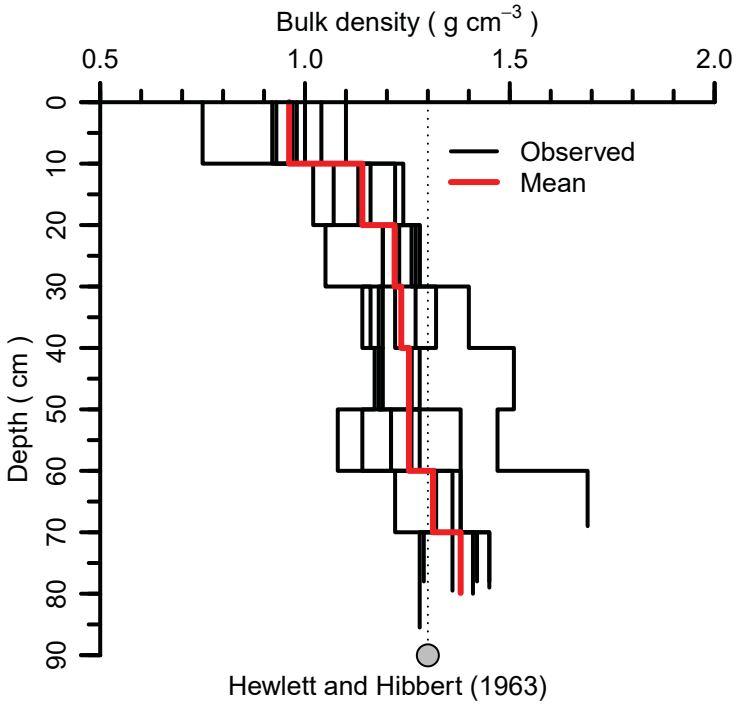
Bulk density (g cm^{-3})
0.5
1.0
1.5
2.0
Depth (cm)
0
10
20
30
40
50
60
70
80
90
Observed
Mean
Hewlett and Hibbert (1963)

Figure3.

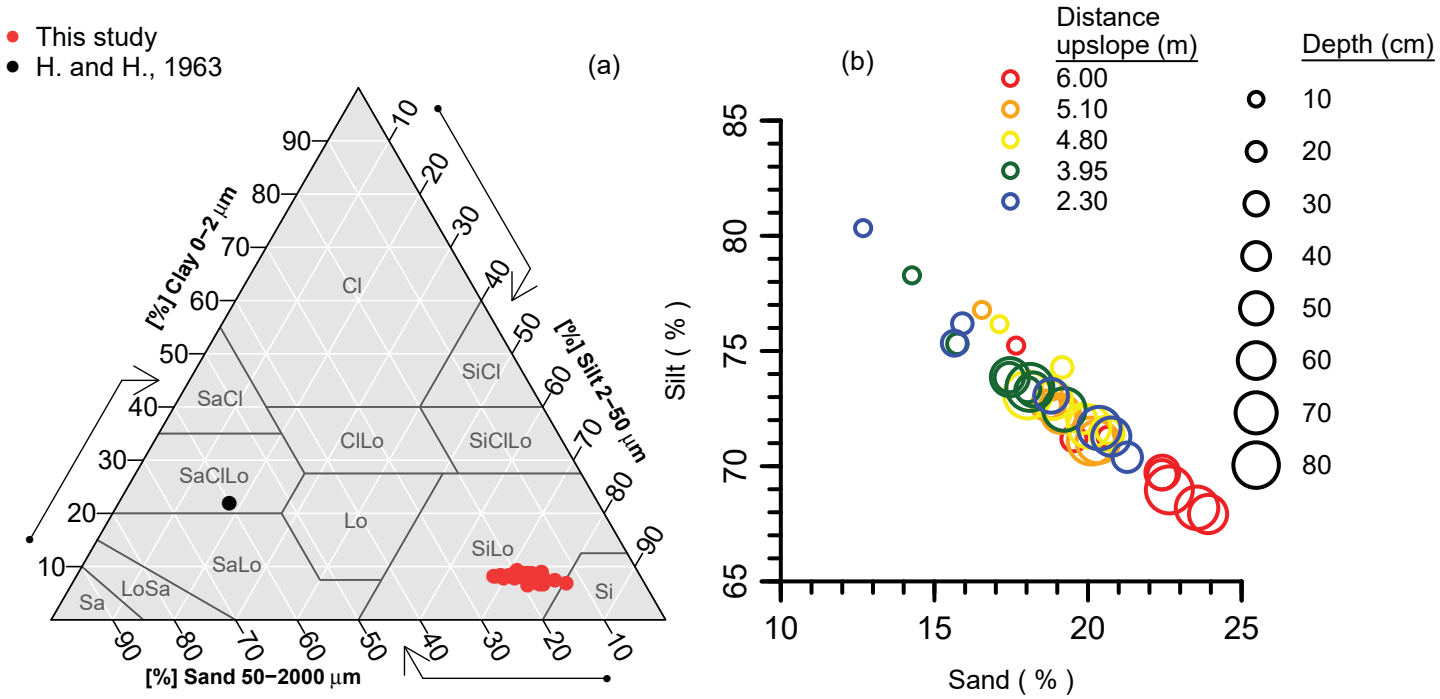
This study
H. and H., 1963
(a)
[%] Clay 0–2 µm
[%] Silt 2–50 µm
[%] Sand 50–2000 µm
Cl
SiCl
SaCl
ClLo
SiClLo
SaClLo
Lo
SiLo
SaLo
LoSa
Sa
Si
(b)
Distance upslope (m)
6.00
5.10
4.80
3.95
2.30
Depth (cm)
10
20
30
40
50
60
70
80
Silt (%)
Sand (%)

Figure4.

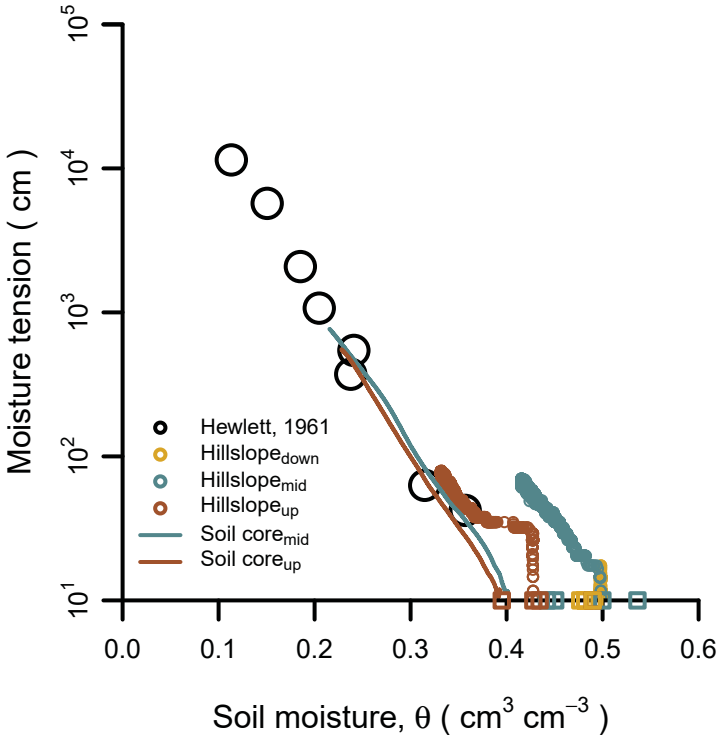
Moisture tension (cm)
10^5
10^4
10^3
10^2
10^1
0.0
0.1
0.2
0.3
0.4
0.5
0.6
Soil moisture, θ (cm^3 cm^{-3})
Hewlett, 1961
$Hillslope_{down}$
$Hillslope_{mid}$
$Hillslope_{up}$
$Soil\ core_{mid}$
$Soil\ core_{up}$

Figure5.

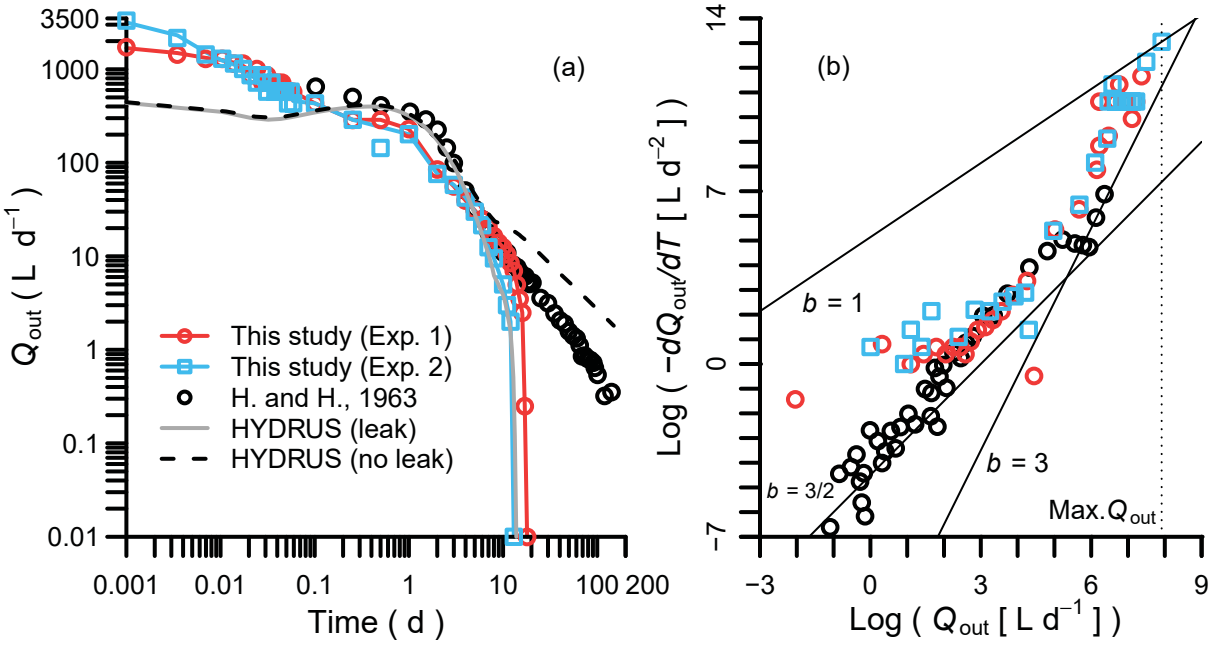
(a)
3500
1000
100
10
1
0.1
0.01
Q_{out} (L d^{-1})
0.001
0.01
0.1
1
10
100 200
Time (d)
This study (Exp. 1)
This study (Exp. 2)
H. and H., 1963
HYDRUS (leak)
HYDRUS (no leak)
(b)
14
7
0
−7
Log ($-dQ_{out}/dT$ [L d^{-2}])
b = 1
b = 3
b = 3/2
Max.Q_{out}
−3
0
3
6
9
Log (Q_{out} [L d^{-1}])

Figure6.

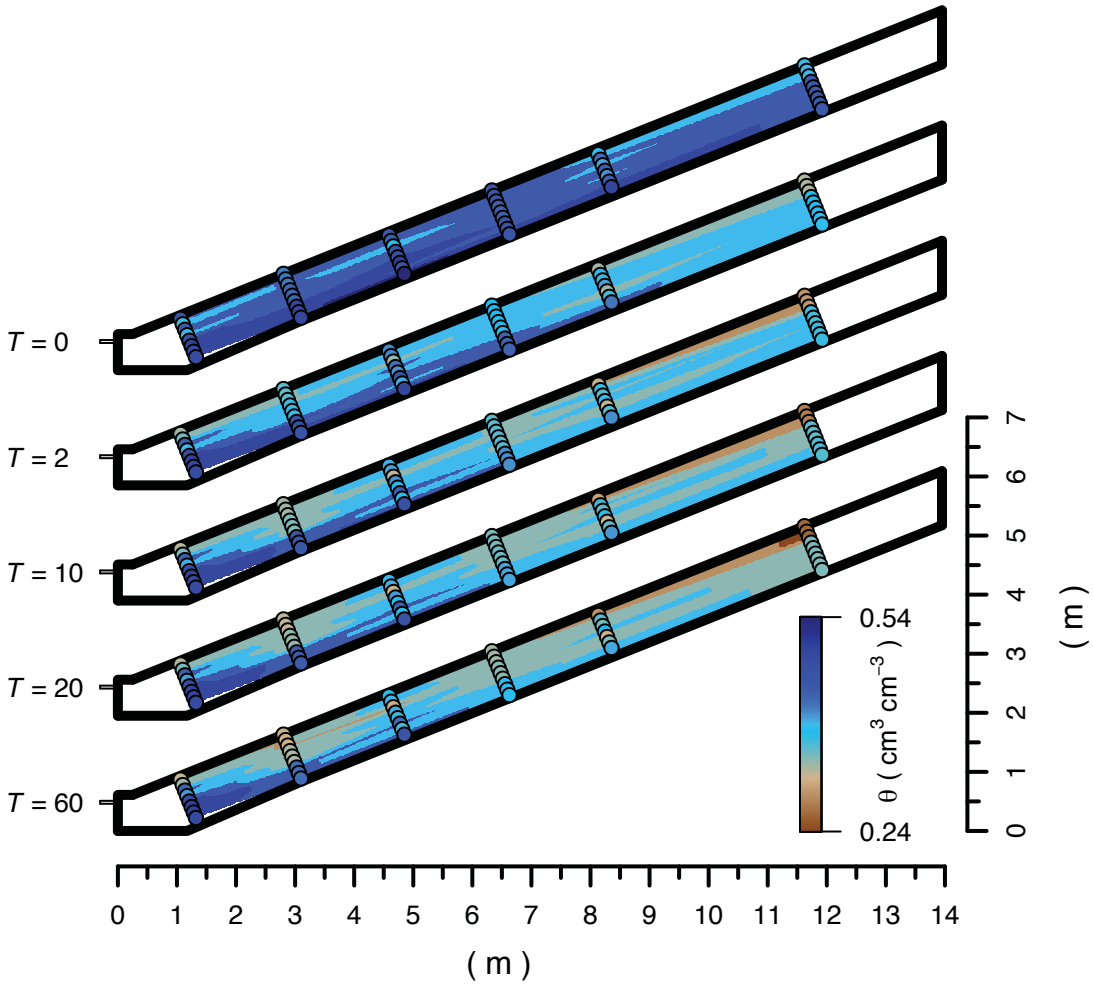
T = 0
T = 2
T = 10
T = 20
T = 60
0.54
θ (cm3 cm−3)
0.24
0 1 2 3 4 5 6 7
(m)
0 1 2 3 4 5 6 7 8 9 10 11 12 13 14
(m)

Figure7.

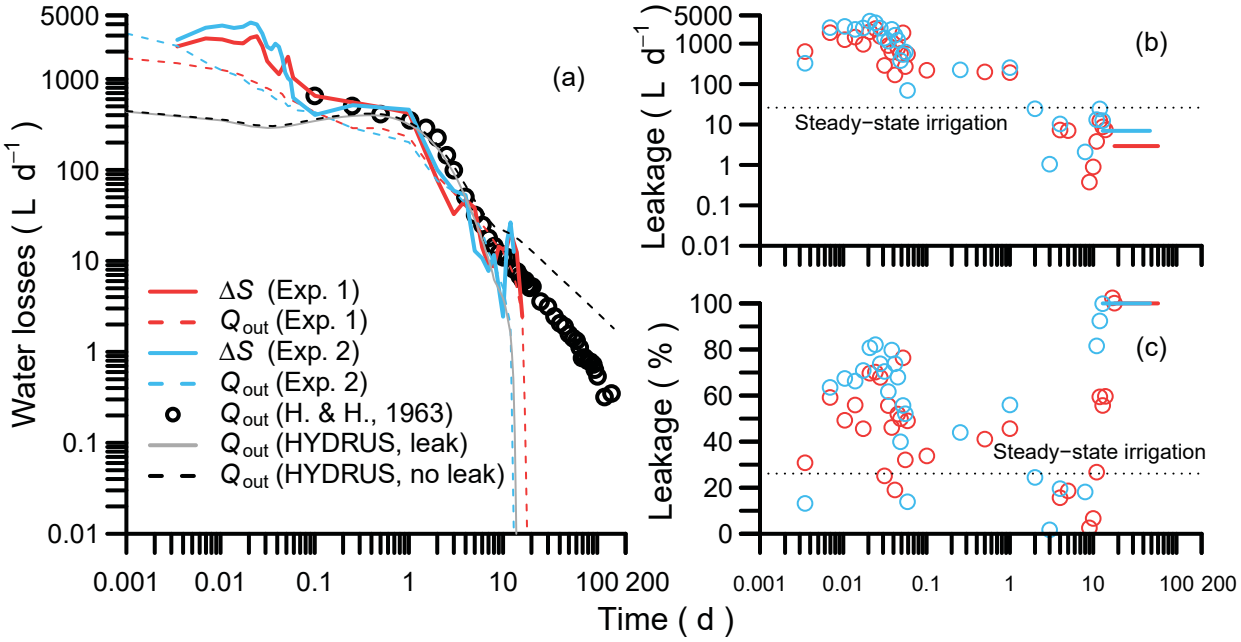
(a)
Water losses (L d^{-1})
5000
1000
100
10
1
0.1
0.01
0.001
0.01
0.1
1
10
100 200
Time (d)
ΔS (Exp. 1)
Q_{out} (Exp. 1)
ΔS (Exp. 2)
Q_{out} (Exp. 2)
Q_{out} (H. & H., 1963)
Q_{out} (HYDRUS, leak)
Q_{out} (HYDRUS, no leak)
(b)
Leakage (L d^{-1})
Steady−state irrigation
(c)
Leakage (%)
100
80
60
40
20
0
Steady−state irrigation

Figure8.

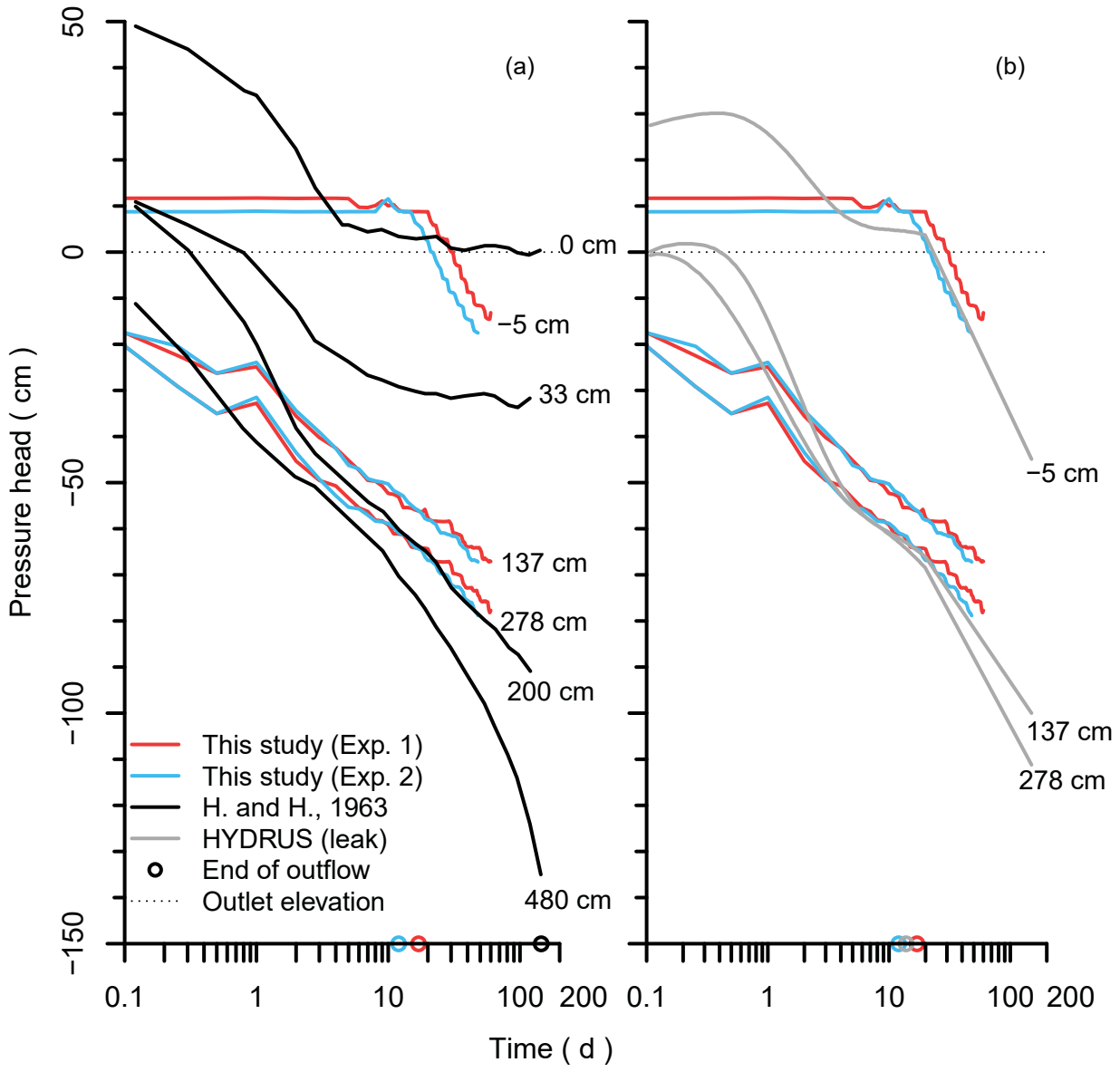
(a)
(b)
Pressure head (cm)
Time (d)
50
0
−50
−100
−150
0.1
1
10
100
200
0 cm
−5 cm
33 cm
137 cm
278 cm
200 cm
480 cm
This study (Exp. 1)
This study (Exp. 2)
H. and H., 1963
HYDRUS (leak)
End of outflow
Outlet elevation

Table 1. *Physical and Hydraulic Properties of Soil in the Physical and Numerical (HYDRUS) Hillslope Models in 1960s and During the Study Period.*

	Previous studies	This study	
		Measured	Modeled
Bulk density (g cm^{-3})	1.3[a]	1.2 (0.02)	
Porosity (%)	50.9[a]	53.4 (0.01)	
Sand (%)	60[a,b]	19.0 (0.3)[c]	
Silt (%)	18[a,b]	72.9 (0.3)[c]	
Clay (%)	22[a,b]	8.1 (0.07)[c]	
θ_r (cm^3 cm^{-3})	0.0[d]	—	0.0
θ_s (cm^3 cm^{-3})	0.49[d]	0.49_D (0.003)[e] 0.50_M (0.02)[e] 0.45_U (0.01)[e]	0.53[e]
K_s (cm h^{-1})	8.4[f]; 8.6[g]; 16.8[h]	10.7_D[i]; 19.7_M[i]; 6.9_U[i]	8.2
a (m^{-1})			3.44
n (—)			1.25

Note: Subscripts (D, M, U) indicate slope position (downslope, midslope, upslope, respectively). Standard errors are given in parentheses.

[a]Hewlett and Hibbert, 1963. [b]Percentage determined by mass using a hydrometer method (Wen et al., 2002). [c]Percentage determined by volume using a laser diffraction method (Konert and Vandenberghe, 1997). [d]Lab values estimated and reported in Hewlett (1961). [e]Means for in situ sensors in the bottom 30 cm of the soil profile at the time of initial drainage for both of our drainage experiments. Each slope location includes data from capacitance-based and TDR-based moisture sensors. The maximum observed value (0.53 cm^3 cm^{-3}) was used in the numerical model. [f]Zecharias and Brutsaert, 1988. [g]Steenhuis et al., 1999. [h]Sloan and Moore, 1984. [i]Cores taken from 10–15 cm depth in the physical model and then analyzed in the lab. The value used in the numerical model was adjusted slightly during calibration after using abovementioned initial estimates from the literature.

Table 2. *Mass Balances of Water and Conservative Tracer (^2H_2O)*

Experiment	Time (d)	S (L)	ΔS from beginning of wetup (L)	Q_{in} (L)	Q_{out} (L)	Water removed during sampling (L)	Residual (L)	(Residual / Cumulative Q_{in}) × 100 (%)
Drainage (1st)	−0.3 (Begin wetup)	3327	(692)	1500	260.0		(548.0)	
	0 (End wetup/begin drainage)	4019	(73)	0	435.5		(731.5)	
	5	3400	41	0	125.5		(720.0)	46.7
	17 (Q_{out} stopped)	3286	167	0	0		(126.0)	
	60 (End experiment)	3160						
	Total		167	1500	821		(846)	
Drainage (2nd)	−0.4 (Begin wetup)	3399	(681)	1500	361.5		(457.5)	
	0 (End wetup/begin drainage)	4080	4	0	397.5		(745.0)	
	5	3395	79	0	53.5		(766.5)	48.5
	12 (Q_{out} stopped)	3320	330	0	0		(251.0)	
	48 (End experiment)	3069						
	Total		330	1500	812.5		(1017.5)	
Drainage (Original[a])	0 (End wetup/begin drainage)	4449[b]			958			
	5				239			
	50				63			
	145 (End experiment)							
	Total				1260			
Steady-state irrigation	0 (Begin irrigation)	3332	(159)	11775	8484.5	(129)	(3002.5)	26.1
	141 (End irrigation)	3491						
	Numerical model (HYDRUS)							29.9
				Tracer input (g)	Tracer collected in outflow	Tracer removed during	Residual (g)	(Residual / Net input) × 100

		(g)	sampling (g)		(%)
^2H_2O tracer	11.06	7.60	(0.21)	(3.25)	30.0

Note: Negative values are given in parentheses. Total residuals for the drainage experiments were calculated for the entire duration of each experiment (from wetup to cessation of Q_{out}) and were not sums of residuals calculated for smaller periods within each experiment.

[a]Hewlett and Hibbert, 1963. [b]Estimated value using soil dimensions from Hewlett and Hibbert (1963) and volumetric soil water content value from the drainage experiment conducted by Hewlett (1961).